

# University of Alberta

High throughput genotyping of single nucleotide polymorphisms in the  
*Plasmodium falciparum dhfr* and *dhps* genes by asymmetric PCR and melt-curve  
analysis

by

Rochelle Emnace Cruz

A thesis submitted to the Faculty of Graduate Studies and Research  
in partial fulfillment of the requirements for the degree of

Master of Science

in

Global Health

Department of Public Health Sciences

©Rochelle Emnace Cruz

Fall 2011

Edmonton, Alberta

Permission is hereby granted to the University of Alberta Libraries to reproduce single copies of this thesis and to lend or sell such copies for private, scholarly or scientific research purposes only. Where the thesis is converted to, or otherwise made available in digital form, the University of Alberta will advise potential users of the thesis of these terms.

The author reserves all other publication and other rights in association with the copyright in the thesis and, except as herein before provided, neither the thesis nor any substantial portion thereof may be printed or otherwise reproduced in any material form whatsoever without the author's prior written permission.

## **Dedication**

For my son,

Casey Cruz

For my parents,

Arlan and Luz Erlinda Emnace

For my grandmothers,

Luisa Banghad and Vicenta Emnace

For my aunts,

the late Corazon Jumaquio and Virginia Emnace Tallo

For my mentor,

Dr. Stephanie Yanow

For my husband, my greatest supporter,

Joseph Cruz

Your unwavering support, guidance, wisdom, and love continue to humble me.

## **Abstract**

Mutations within *Plasmodium falciparum* dihydrofolate reductase (*pfdhfr*) and dihydropteroate synthase (*pfdhps*) genes contribute to resistance to antimalarials such as sulfadoxine-pyrimethamine (SP). Single nucleotide polymorphisms (SNPs) within codons 51, 59, 108 and 164 in the *pfdhfr* gene and codons 436, 437, 540, 581, and 613 in the *pfdhps* gene are associated with SP treatment failure. This study focused on the development of a genotyping assay based on asymmetric real-time PCR and melt-curve analysis. Probes specific to each SNP hybridize differentially to mutant and wild-type sequences, generating distinct melting curves. The analytical sensitivity and specificity were determined on the LightCycler® platform using reference strains of malaria. The assay was validated with clinical samples from patients with malaria and compared to a gold standard test. This assay was also tested for its application to in-gel PCR technology for point-of-care testing in resource-limited areas. Genotyping is possible with further enhancements to this technology.

## **Acknowledgements**

The completion of this thesis would have not been possible without the contribution and support from several people who I owe my deepest gratitude.

First and foremost, I would like to sincerely thank my supervisor, Dr. Stephanie Yanow, who has given me the greatest opportunity I can ever imagine. Her support and guidance is limitless, and her passion to learn is contagious. I am forever grateful.

Second, I would like to thank all the support that I have received from Specialized Support and Disability Services at the University of Alberta. Their guidance and patience have given me a renewed outlook on learning.

Finally, I am indebted towards Sandy Shokoples, Amy Delorme, Ann Edwards and Jana Lauzon, who have helped me with the technical support and assistance with any laboratory work. I am also thankful for all the support from Team Microfluidics. I especially want to thank Dr. Dammika Manage, Dr. Alexey Atrazhev, Dr. John Crabtree, Dr. Brian Taylor, Ayo Olanrewaju, Kim Martin, YC Morrissey, and Alex Stickel.

## Table of Contents

Dedication .....	II
Abstract .....	III
Acknowledgements .....	IV
List of Figures .....	VII
List of Tables.....	IX
Chapter 1: Introduction.....	1
1.1 Antimalarial treatment.....	2
1.1.1 History of antimalarial agents.....	2
1.1.2 Antimalarial agents .....	4
1.1.2.1 Quinine.....	4
1.1.2.2 Chloroquine .....	4
1.1.2.3 Sulfadoxine-pyrimethamine .....	5
1.2 Emergence of drug resistance .....	7
1.2.1 History.....	7
1.2.2 Etiology of resistance .....	8
1.2.2.1 Selective drug pressure.....	9
1.2.2.2 Compliance .....	10
1.2.2.3 Sub-standard drugs .....	11
1.2.3 Biological mechanism of resistance .....	12
1.3 SP use for IPTp.....	13
1.3.1 Presumptive treatment in pregnancy .....	13
1.3.2 SNPs associated with treatment failure .....	15
1.3.3 Analysis of treatment failure.....	18
1.3.4 Need for surveillance of SP-resistance.....	21
1.4 Methods of molecular surveillance for SP.....	21
1.4.1 Monitoring of parasite drug resistance.....	21
1.4.2 Molecular tests .....	21
1.4.2.1 Real-time PCR technology .....	22
1.4.2.2 TaqMan® minor groove binding probes .....	23
1.4.2.3 Intercalating DNA-binding dyes .....	24
1.4.3 High-throughput genotyping using asymmetric PCR and MCA .....	24
1.4.4 Application onto a “nano” device .....	27
1.5 Hypothesis .....	27
1.5.1 Objectives/research question .....	28
1.5.2 Study aims .....	28
Chapter 2 LightCycler® assay.....	29
2.1 Introduction .....	29
2.2 Materials and methods.....	31
2.3 Results .....	37
2.3.1 Sensitivity of melt-curve analysis for genotyping <i>pf dhfr</i> .....	37
2.3.2 Sensitivity of melt-curve analysis for genotyping <i>pf dhps</i> .....	42
2.3.3 Evaluation of MCA with clinical samples.....	46
2.3.4 Comparison of MCA and Taqman PCR for genotyping <i>pf dhfr</i> .....	50
2.4 Discussion.....	51

Chapter 3 Application of the MCA assay to in-gel PCR technology .....	55
3.1 Introduction.....	55
3.2 Materials and methods.....	56
3.2.1 DNA template.....	56
3.2.2 In-gel PCR of <i>pfdhfr</i> codon 108.....	56
3.2.3 Polymerization of PCR reagents .....	57
3.2.4 PCR process.....	58
3.3 Results .....	60
3.3.1 LightCycler® in-gel PCR.....	60
3.3.2 Genotyping from in-gel PCR on the LightCycler® .....	62
3.3.3 In-gel PCR on the Viriloc .....	63
3.3.4 Ramping rates .....	64
3.3.5 Gel concentration .....	69
3.3.6 Unpolymerized polyacrylamide inhibition.....	70
3.3.7 Annealing temperatures.....	71
3.3.8 Hairpin structures.....	72
3.4 Discussion.....	73
Chapter 4: Discussion and conclusions .....	78
4.1 Application of the LightCycler® assay for surveillance .....	78
4.1.1 Building laboratory capacity in Uganda.....	80
4.1.2 Surveillance programs in Uganda .....	82
4.2 General conclusions regarding the in-gel technology .....	85
4.2.1 Limitations of the system .....	86
4.2.2 Technological requirements for change .....	87
4.2.3 Future implications: application of the technology for use in the field.....	88
References .....	94
Appendix 1: Glossary .....	102

## List of Figures

Figure 1.1 Lifecycle of malaria and the target sites for antimalarials. ....	2
Figure 1.2 Enzymes and substrates involved in the folate pathway and the target sites for sulfadoxine and pyrimethamine.. ....	6
Figure 1.3 Proposed burden of parasites in pregnant women taking SP-IPTp in areas of high transmission. ....	14
Figure 1.4 Pyrimethamine-inhibitor interactions at the active site of the DHFR enzyme with the mutations associated with resistance .....	16
Figure 1.5 Sulfadoxine-inhibitor interactions at the active site of the DHPS enzyme with the mutations associated with resistance. ....	17
Figure 1.6 Melting peak profiles for wild-type and mutant sequences. ....	26
Figure 2.1 Genotyping of SNPs in the <i>pfdhfr</i> gene by asymmetric PCR and melt-curve analysis. ....	39
Figure 2.2 Genotyping of SNPs in the <i>pfdhps</i> gene by asymmetric PCR and melt-curve analysis. ....	43
Figure 2.3 Melting curve plot of one of the clinical samples with a mixed genotype (green) at codon 108 overlaid with melt curves from samples with the wild-type (blue) and mutant (red) SNPs.....	49
Figure 3.1 Schematic of (A) gel post arrays and (B) the Viriloc system, which is the prototype instrument used to perform in-gel PCR and MCA. <i>Figures adapted from Atrazhev et al. (2010)</i> . ....	58
Figure 3.2 Melting curve plots of replicate reactions of in-gel PCR performed on the LightCycler® for <i>pfdhfr</i> at codon 108 using 3D7 plasmid DNA. ....	61
Figure 3.3 Melting curve plots from genotyping at SNP S108N of the <i>pfdhfr</i> gene by in-gel PCR performed within the LightCycler® capillaries.....	62
Figure 3.4 Melting curve profiles and gel electrophoresis of in-gel PCR products following amplification and melt curve analysis on the Viriloc. ....	63
Figure 3.5 Melting curve plots of asymmetric in-gel PCR without (A) and with (B) probe performed on the Viriloc. Products that melt at 80 °C correspond to full-length amplicons (AD= amplicon duplex peak), whereas primer-dimers melt at 73 °C. ....	64

- Figure 3.6 Melting curve profiles from in-gel PCR of a plasmid with the wild-type sequence at codon 108 in the *pfdhfr* gene performed in capillaries on the LightCycler® tested with the Viriloc ramp rate settings for (A) symmetric and (B) asymmetric PCR without probes. AD = amplicon duplex peak; PD = primer-dimer peak..... 66
- Figure 3.7 Melting curve plots to genotype *P. falciparum* plasmid DNA with the wild-type (S108) and mutant (108N) sequences using the Viriloc ramp rate settings on (A) the Lightcycler® and (B) the Viriloc system. S = wild-type at codon 108; N = mutant at codon 108..... 68
- Figure 3.8 Gel electrophoresis of the asymmetric PCR reaction of plasmid DNA with the wild-type sequence for amplification of *pfdhfr* SNP S108 using an excess of the reverse primer performed on the gradient thermocycler. .... 72
- Figure 3.9 Melting curve profiles for asymmetric in-gel PCR of plasmid DNA with the wild-type sequence for *pfdhfr* SNP 108 with an excess of the forward primer tested on the LightCycler®..... 73



## List of Tables

Table 2.1 <i>Dhfr</i> and <i>dhps</i> haplotypes for <i>P. falciparum</i> strains and plasmid.....	33
Table 2.2 Primer and probe sequences for the SNPs in the <i>pfdhfr</i> and <i>pfdhps</i> genes .....	35
Table 2.3 Pyrosequencing primers.....	37
Table 2.4 Analytical sensitivity of the genotyping assay for each SNP in the <i>pfdhfr</i> gene using MCA.....	40
Table 2.5 Limit of detection for <i>pfdhfr</i> SNP identification by MCA.....	41
Table 2.6 Dynamic range of genotyping assay for <i>pfdhfr</i> using serially diluted wild-type cultures .....	42
Table 2.7 Analytical sensitivity of the genotyping assay for each SNP in the <i>pfdhps</i> gene using MCA.....	44
Table 2.8 Limit of detection for <i>pfdhps</i> SNP identification by MCA .....	45
Table 2.9 Dynamic range of genotyping assay for SNPs in the <i>dhps</i> gene using a serially diluted <i>P. falciparum</i> strain 3D7.....	46
Table 2.10 Concordance between the MCA and TaqMan assays for the SNPs in the <i>pfdhfr</i> gene compared against the gold standard.....	48
Table 2.11 Concordance between the MCA assay and the gold standard for genotyping the SNPs in the <i>pfdhps</i> gene.....	50
Table 3.1 Summary of factors that contribute to the generation of primer-dimers. .....	70

## List of abbreviations

ABCs	azithromycin-based combination
ACTs	artemisinin-based combination therapy
CDC	Centers for Disease Control and Prevention
CQ	chloroquine
DNA	deoxyribonucleic acid
FP	ferriprotoporphyrin IX
FRET	fluorescence resonance energy transfer
HRM	high resolution melting
IPTp	intermittent preventative therapy for pregnancy
MCA	melting-curve analysis
MGB	minor groove binding probe
MIC	minimum inhibitory concentration
PCR	polymerase chain reaction
<i>pfcr1</i>	gene encoding <i>P. falciparum</i> chloroquine resistance transporter
<i>pfdhfr</i>	gene encoding <i>P. falciparum</i> dihydrofolate reductase
<i>pfdhps</i>	gene encoding <i>P. falciparum</i> dihydropteroate synthase
<i>pfmdr</i>	gene encoding <i>P. falciparum</i> multidrug resistance protein
POC	point-of-care testing
RFLP	restriction fragment length polymorphism
SNPs	single nucleotide polymorphism
SP	sulfadoxine-pyrimethamine
UMSP	Uganda Malaria Surveillance Project
UVRI	Uganda Virus Research Institute
WHO	World Health Organization

## Chapter 1: Introduction

“So long as Woman has walked the Earth, malaria may have stalked her.”

*Patrick Duffy*

Malaria is one of the leading causes of death and disease in many developing countries. In 2009, the CDC reported between 190 and 311 million clinical episodes worldwide (84). Despite ongoing efforts to eradicate malaria, the WHO reported that the death toll due to malaria ranges from 708,000 to 1,003,000 annually; approximately 89% of these deaths occur in Africa (84).

Malarial disease originates from the inoculation of the parasite *Plasmodia* into the human host through an infectious bite of the female *Anopheles* mosquito carrying the sporozoite form of the parasite (Figure 1.1). Sporozoites travel through the blood to the liver and infect hepatocytes. During this stage, the parasite is likely to incur *de novo* polymorphisms during DNA replication and schizogony in the liver. The merozoites produced from the liver stage enter the bloodstream to infect erythrocytes, which culminates in the clinical presentation of malaria. Parasites go through multiple cycles of multiplication and infection of new red blood cells, giving rise to further polymorphisms in the parasite genome. In this stage, some merozoites will differentiate into gametocytes, the sexual forms of the parasite, which will eventually be ingested by the mosquito vector, mature into the sporozoite form and further propagate the disease. There are five species of *Plasmodia* that cause malaria in humans: *P. falciparum*, *P. vivax*, *P. ovale*, *P. malariae*, and *P. knowlesi*. Regardless of which species infects the host, there is only one sporozoite required to cause disease, characterized by symptoms

of fever, chills, mild anemia, malaise, and abdominal discomfort (79). Of the five species, *P. falciparum* is the most virulent form; without proper treatment, people infected with this species can lapse into a coma or potentially die (13).

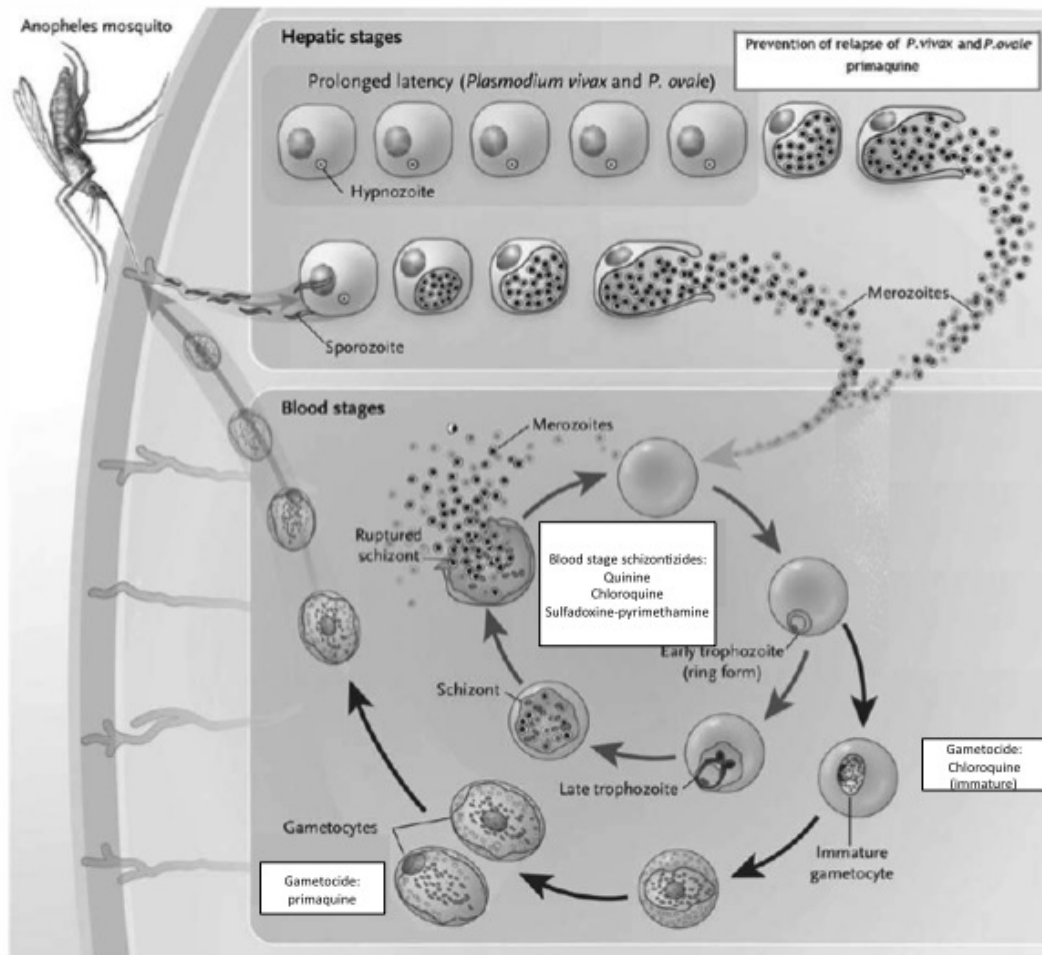


Figure 1.1 Lifecycle of malaria and the target sites for antimalarials. *Adapted figure from Daily (2006).*

## 1.1 Antimalarial treatment

### 1.1.1 History of antimalarial agents

As early as 2700 BCE, symptoms of malaria were documented in ancient Chinese writings. In the second century BCE, the remedy for fever was the active

ingredient of Qinghao, which is presently known as artemisinin. Prior to the 20<sup>th</sup> century, the best effective treatment for “cessation of febrile paroxysms” was quinine, which was first described in 1632 (1). Spanish Jesuit priests in Peru were introduced to the medicinal properties of the Cinchona plant by South American Indigenous people, who were the first to recognize that this agent could be extracted from the tree bark, and prepared into a powdered mixture that was ingested with wine (1). The active ingredient from the bark would be later known as quinine, an antimalarial that is still used four centuries later.

The movement towards developing synthetic antimalarial drugs was prompted by a lack of access to quinine. After World War II, chloroquine (CQ), a 4-aminoquinoline chemotherapeutic agent, became the preferred first line treatment for malaria (18). Similarly, CQ was used as a presumptive treatment of fevers. Its low cost and minimal side effects encouraged massive drug distribution by medicating cooking salt with CQ (60). This method for malaria control offered a potential solution to problems with compliance and adherence to drug treatment. However, indiscriminate use of the drug created selective pressure on the parasite population, contributing to the selection of resistant strains, and once again the world was in need of an effective therapeutic drug for malaria.

During the 1950s, sulfa drugs became increasingly popular as antimalarials; however, the toxicity profiles required improvement. At the same time, an efficacy study of pyrimethamine looked at the influence of weekly prophylaxis on children for a period of one year (15, 28). Unfortunately, after the course of the year, resistance to the drug became evident. By 1959, a study

showed that the synergistic effect of sulfadoxine and pyrimethamine was superior in clearing *P. falciparum* infections (27, 28). The curative effects of sulfadoxine-pyrimethamine (SP) combination treatment were widely accepted in endemic countries (28). By the early 1990s, many malaria endemic countries in sub-Saharan Africa were faced with the declining efficacy of CQ, and this prompted health policy changes to advocate the use of SP as the front-line treatment. However, within a year of implementation, sensitivity to the drug began to decline, indicating that SP would not be an effective treatment in the long-term (61). Despite the rapid emergence of resistance against SP, many affected countries in sub-Saharan Africa continue to utilize SP during pregnancy with intermittent preventative therapy (IPTp).

## **1.1.2 Antimalarial agents**

### **1.1.2.1 Quinine**

Quinine is one of the oldest chemotherapeutic agents, and it causes parasite cell lysis through the disruption of parasite membrane function. Quinoline antimalarials, such as quinine, accumulate within the digestive vacuole of the parasite and inhibit haemozoin formation by binding of the agent to ferriprotoporphyrin IX (FP) (22, 61). This blood stage schizonticide is effective in killing trophozoites in the red blood cells. Quinine is ineffective against parasites present in the exo-erythrocytic stage in the liver.

### **1.1.2.2 Chloroquine**

Like quinine, chloroquine (CQ) is categorized as a quinoline antimalarial that causes morphological changes within the parasite. The morphological effects

of CQ differ from quinine. The former allows for the build up of hemoglobin transport vesicles whereas the latter does not (19). Similar to quinine, CQ causes its deleterious effects by binding to FP which leads to the toxic accumulation of heme molecules within the parasite (22, 23). The parasite utilizes FP to form the non-toxic malarial pigment, hemozoin. This chemotherapeutic antimalarial has blood stage schizonticidal activity against *Plasmodium spp.* and gametocytocidal activity particularly against *P. malariae*, *P. ovale*, and *P. vivax*. Intensive distribution of CQ through malaria control programs have contributed to many strains of *P. falciparum* developing genetic mutations that limit the accumulation of the drug within the parasite vacuole, rendering it drug-resistant (70). Given the rapid spread of resistance, many countries in Africa adopted SP as their first line of treatment against uncomplicated malaria.

### **1.1.2.3 Sulfadoxine-pyrimethamine**

SP is a combination drug wherein both of the active ingredients affect the folate pathway. Sulfadoxine is a sulfa drug that inhibits the dihydropteroate synthase (DHPS) enzyme, and pyrimethamine inhibits the dihydrofolate reductase (DHFR) enzyme (28). Collectively, these enzymes are necessary for the reduction of folate, which is an essential co-factor for DNA synthesis (Figure 1.2) (28, 33, 76). The inhibition of DHFR and DHPS causes the depletion of dTMP and dTTP, respectively, thereby decreasing parasite DNA synthesis (33, 76). The exogenous addition of SP is most toxic during the late erythrocytic stage, which is the peak of DNA synthesis (13, 28). This chemotherapeutic agent is thought to induce the early release of gametocytes, thereby producing an immature form

with reduced infectivity (9). This reduced infectious form is ideal for limiting the spread of disease, however, gametocyte density is found to increase in parallel with SP resistance (9).

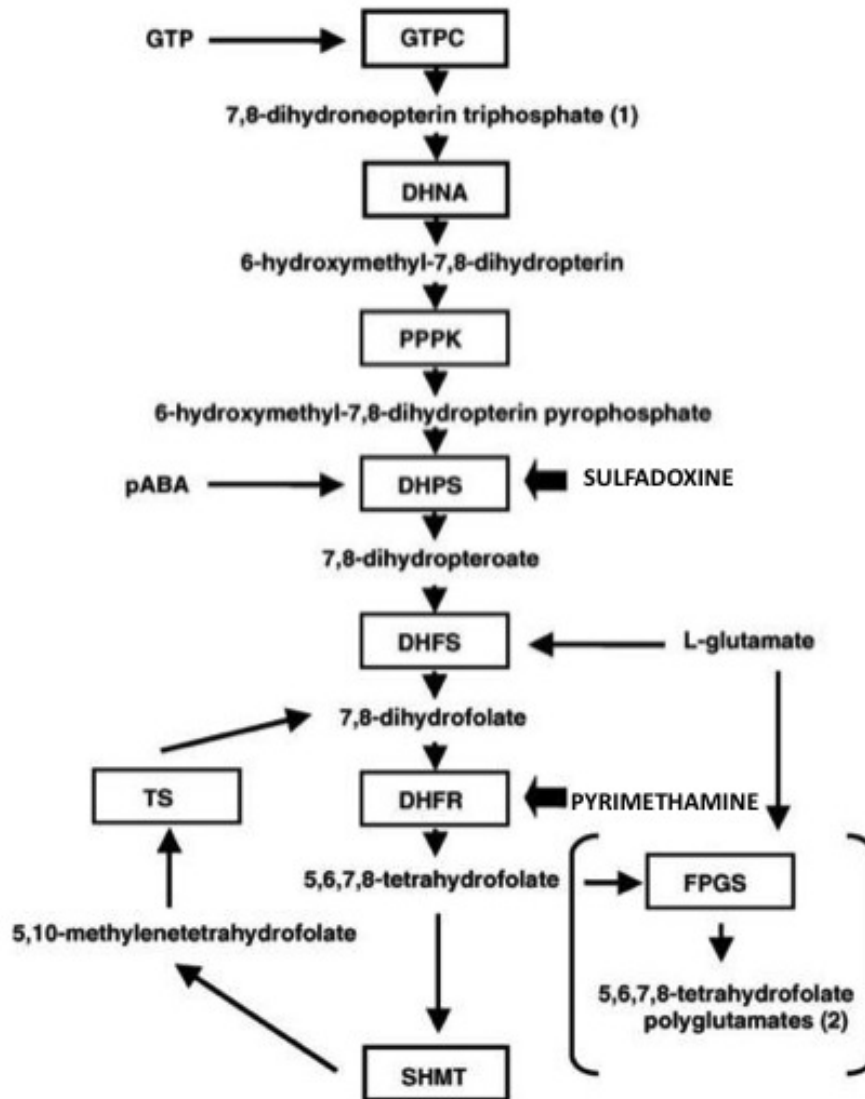


Figure 1.2 Enzymes and substrates involved in the folate pathway and the target sites for sulfadoxine and pyrimethamine. *Figure adapted from Hyde (2005).*

SP has a relatively long half-life, which allows the drug to persist within the host, eventually at sub-standard drug concentrations. In healthy, non-pregnant



women, the mean elimination half-lives are 200 and 100 hours for sulfadoxine and pyrimethamine, respectively. Pregnancy alters the pharmacokinetics of any drug, including SP, which complicates the process of determining the sufficient dosage given to women for prophylaxis (53, 55).

## **1.2 Emergence of drug resistance**

### **1.2.1 History**

Parasite resistance is described as the ability of a parasite “to survive and/or multiply despite the administration and absorption of a drug in doses equal to or higher than those usually recommended but within the limits of tolerance of the subject” (12, 76). The first records of resistance against quinine appeared in 1908 in Brazil (28). Amazingly, the long-standing use of quinine has not culminated in widespread resistance, which may be attributed to its short half-life of 8 -10 hours (61). The efficacy of quinine has remained consistent from the 1970s to the early 2000s. The degree of resistance against quinine is conventionally low-grade, whereby drug activities are either delayed or lessened (1). Unfortunately, the same low level and slow spread of resistance cannot be said about other antimalarials, such as CQ and SP.

The global malaria eradication campaigns of the 1950s and 1960s were intended to eliminate malaria through the widespread distribution of CQ and spraying with dichlorodiphenyltrichloroethane (DDT) (76). By 1962, CQ resistance was rampant across Southeast Asia and South America (54). Resistance to CQ was firmly established in sub-Saharan Africa by 1989 (54). An inability to sustain the eradication program led to the abandonment of malaria control, which then led to the resurgence of malaria in many countries (21). Despite the

inefficacy of CQ created by resistance, the antimalarial was still widely used because the low cost of treatment was a financial incentive that many countries could not relinquish (28).

### **1.2.2 Etiology of resistance**

“Parasite resistance” is often confused with the term “treatment failure” because of the similarities in their outcomes. It is important to understand that the two terms are not synonymous, as a person can suffer treatment failure even when the parasite itself does not have any polymorphisms that confer resistance to the drug. Likewise, a parasite can have certain genetic mutations associated with resistance *in vitro*, while the patient may not necessarily experience treatment failure. The current definition for treatment failure is the presence of parasitemia at either Day 3 (Early Treatment Failure) or Day 14 (Late Treatment Failure) from follow-up (82). This outcome can be caused by any of the following mechanisms: parasite drug resistance, poor adherence to antimalarials, sub-standard medicine, or inadequate drug exposure due to incorrect dosing (82). Drug resistance refers to the parasites that are able to persist after treatment. Increases in parasitemia can also be attributed to the attack of sequestered schizonts; however decreases in parasitemia could be due to the sequestering of parasites. Resistance can go unrecognized without the invaluable results from clinical drug trials, *in vivo* and *in vitro* testing, and molecular typing (12).

### 1.2.2.1 Selective drug pressure

In regions with high rates of transmission, the generalized symptoms of malaria frequently mislead many physicians to assume that a patient is suffering from malaria. Rather than performing a test to confirm the infection, physicians automatically prescribe an antimalarial for treatment. The over-use of antimalarials generates selective drug pressure that results in the proliferation of parasites with certain molecular mutations that enable them to grow in the presence of the drug. Presumptive self-treatment by patients living in malaria-endemic areas also contributes to this selective drug pressure. One problem associated with self-medication is potential under-dosing and sub-optimal drug concentrations in a patient suffering from malaria (46).

The development of resistant mutations has been associated with the loss of fitness. Thus, when the selective drug pressure is removed, resistant parasites will be outgrown by drug-sensitive parasites. One might predict that CQ-sensitive parasites would increase in prevalence in countries that banned the use of CQ. Malawi was the first country to experience the reemergence of CQ-sensitive malaria 12 years after the cessation of CQ use in 1993 (38, 40). The results of the *in vitro* study by Kublin *et al.* (2003) indicate that removal of selective drug pressure can potentially reduce the prevalence of resistant parasites (38). Unfortunately, this reversion to CQ-sensitive *P. falciparum* was not observed in Kilifi, Kenya (52). Despite a ban on its use in Kilifi, CQ was still available for self-medication in neighboring communities. The reintroduction of the drug back into the community of Kilifi will be delayed to allow the decline in resistant

strains. The slow decrease in resistance that was experienced in coastal Kenya is an example of the importance of drug policy implementation, compliance, and surveillance.

#### **1.2.2.2 Compliance**

Antimalarial compliance is largely a reflection of the ability of a patient to follow prescribed dosing with medication. Resistance has been associated with a lack of compliance, as many people do not complete the course of treatment (12). Cost, adverse side effects, and frequency of administration are factors that affect willingness to adhere to a drug schedule. A study on drug combination efficacy and adherence in rural Senegal observed that families often stop treatment once the symptoms have ceased (74). In the same study, approximately 35% of children did not receive the recommended dose and 62% did not demonstrate adherence to the schedule. Although the symptoms may stop, the parasite can potentially grow under conditions in which the drug levels are too low to be effective. This low drug level can potentially select for the drug resistant parasites to proliferate. Souares *et al.* (2008) suspect that this poor adherence is attributed to increased efficacy with rapid loss of symptoms encouraging caregivers to stop providing treatment. This poor compliance can also be attributed to the lack of training of health professionals in how to inform patients about their treatment.

Although most of the problems associated with compliance are directed towards the patient, the people responsible for dispensing the drugs and instructing the patients on the appropriate use also contribute to the rise in resistance. There have been reports that many privatized pharmacies in sub-

Saharan Africa are unaware of antimalarial dispensation policies; this leads to inappropriate treatment as well as poor instructions on how to use the medication (26). In this context, “inappropriate treatment” entails inadequate drug dosage, incorrect drug type, and poor quality. Medicine sellers permit the easy access to antimalarials, including those that require a prescription. Unfortunately, the information provided at the time of dispensation varies widely. Consequently, this leads to misinformed customers taking inadequate dosages. Pharmacies located in rural areas of Burkina Faso also demonstrated that self-medication with either CQ or SP is commonly practiced, but that underdosing will result in resistance against the antimalarial (63). One remedy to this problem is to ensure that the pharmacies responsible for dispensing antimalarials are providing suitable instructions to the patients for them to be effective. However, enforcing dispensing regulations for medicine sellers is not feasible, as effective malaria control requires buy-in from the community, shopkeepers, and governing bodies.

### **1.2.2.3 Sub-standard drugs**

Drugs are only effective if they are used appropriately. While this is true if the patient adheres to the instructions of use, efficacy is also dependent on the quality of the drug. Counterfeit and substandard drugs are becoming as widespread as the disease itself. The consequence of using counterfeit antimalarials is an increase in morbidity and mortality caused by the infection. This dispersal of poor quality drugs is encouraging the spread of resistance by enabling the parasite to survive at sub-inhibitory drug concentrations (11). In a study of antimalarial drug quality across six African countries, the failure rate for

meeting internationally acceptable standards for SP ranged from 27% to 50% (11). Counterfeit drugs are especially prevalent in poorer countries, due to the lack of regulatory systems.

### **1.2.3 Biological mechanism of resistance**

Effective antimalarials target pathways that prevent proliferation and transmission of the parasite. Genetic mutations that allow the parasite to survive in the presence of the antimalarials lead to resistance. Resistance against CQ is multigenic as certain mutations within the *pfcr*t and *pfmdr* genes allow the parasite to evade drug toxicity by expelling the drug out of the digestive vacuole of the parasite (13). The exact mechanism to reduce the accumulation of the drug is still unknown. However, parasites with these mutations have a lower level of fitness (38); in the absence of selective pressure, *Plasmodium* strains sensitive to drugs will outgrow the parasites with mutations (65).

SP has the functional ability to inhibit *de novo* synthesis of nucleotides and amino acids in *Plasmodia*, thus halting their life cycle (70). In SP-sensitive strains of *P. falciparum*, the DHFR and DHPS enzymes bind to the agent, which then prevents the synthesis of pyrimidines. As mentioned previously, resistance develops in protozoa with mutations that enable them to grow in the presence of inhibitory concentrations of the drug. In this situation, resistance is generated by point mutations that alter the configuration of the SP binding site for the enzyme. It is postulated that the polymorphisms associated with SP resistance cause conformational changes that sterically impede the binding of the drug (58). The molecular markers that are associated with resistance are described as single-

nucleotide polymorphism (SNPs). These SNPs will be discussed in detail in the subsequent section.

### **1.3 SP use for IPTp**

#### **1.3.1 Presumptive treatment in pregnancy**

Widespread resistance to SP has driven many endemic areas to change the national policy on the frontline treatment of uncomplicated malaria and many areas now utilize artemisinin-combination therapies (ACTs) as the first line therapy. However, SP remains widely accepted as a presumptive treatment for pregnant women. This prophylaxis regimen, known as intermittent preventative treatment in pregnancy (IPTp), entails the administration of SP as a prophylaxis during the second and third trimesters (72). The benefits of this intervention include a reduction in morbidity associated with placental malaria, a reduction in maternal anemia and an increase in birth weight (59). When selecting a drug for IPTp, it is important to consider the half-life of the drug and the existing levels of resistance (56). Other antimalarials such as amodiaquine and mefloquine have low tolerability but they are still promising candidates to replace SP for IPTp (72). Although other drugs are considered safe for pregnant women, SP is considered the best option because of its long half-life. The prolonged half-life of SP clears current infections and also prevents subsequent infections. However, in high transmission areas, resistance against SP compromises the prophylactic effect by shortening the period of efficacy (Figure 1.3) (81).

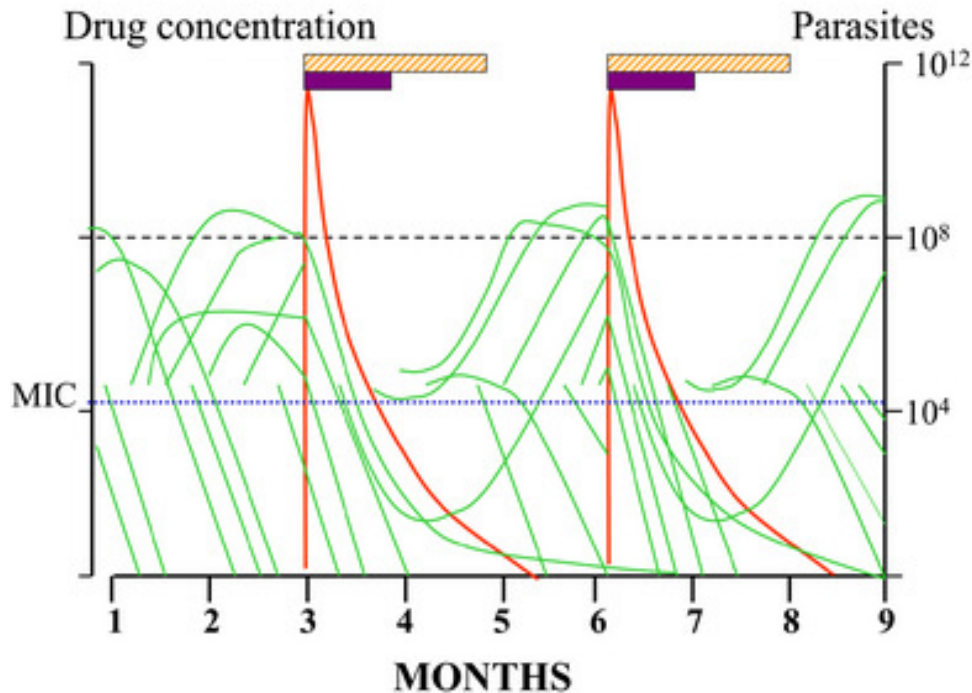


Figure 1.3 Proposed burden of parasites in pregnant women taking SP-IPTp in areas of high transmission. Each green line depicts an infection, the hatched bars represent the suppressive prophylactic activity and the solid purple bar represents the period during which parasite multiplication is inhibited. *Figure adapted from White et al. (2005).*

Immunity plays a significant role in the elimination and inhibition of parasite growth (79). The weaker immune response during pregnancy reduces the efficacy of antimalarials. Similarly, the pharmacokinetics of SP changes during the later stages of pregnancy, thereby altering post-treatment prophylaxis.

Absorption of SP is reduced during pregnancy, due to a decrease in gastric emptying (59). The WHO reported that the present state of SP use fails to reach the >95% cure rate (48, 82). Widespread resistance prior to the implementation of IPTp programs creates uncertainty in the use of SP for chemoprophylaxis.

However, alternative antimalarials, such as the mefloquine and azithromycin-



based combinations (ABCs), approved for pregnancy do not have the same level of tolerability as SP (72). Both mefloquine and ABCs are the leading candidates for the replacement of SP for IPTp (14). Clinical drug trials systematically exclude pregnant women from being studied despite the fact that *in vivo* studies play an important role in understanding drug efficacy among pregnant women living in high transmission areas.

### **1.3.2 SNPs associated with treatment failure**

The unique genomic characteristics, such as the A-T rich DNA sequences, of *Plasmodia* have enabled both their survival and evasion from host elimination (7). The recombination rate in *P. falciparum* has been of strong interest to those studying the origins of resistance and mutations associated with reduced antimalarial sensitivity. These rates vary among the different strains of *P. falciparum* but also within various chromosomes (35). Genetic recombination reaches its peak during sexual recombination of the gametocytes in the midgut of the mosquito vector. This sexual stage enhances the generation of drug resistant strains. Since SP is ineffective against gametocytes, the sexual forms, any surviving gametocytes with polymorphisms associated with resistance will eventually pass on these genetic traits to the sporozoites. Consequently, areas of high malaria transmission will experience high recombination rates (45).

High mutation rates lead to the accumulation of SNPs (61). Reduced sensitivity against pyrimethamine has been associated with mutations at codons 50, 51, 59, 108, and 164 in the *dhfr* gene (79). Pyrimethamine competes with the natural substrate H<sub>2</sub>folate (DHF) for the active site of the enzyme. These SNPs

result in substitutions in the amino acid side chain, which prevent binding of pyrimethamine to the active site (Figure 1.4) (43, 58, 90). Mutation at codon 108 is perceived to be the first of the stepwise accumulation of SNPs that leads to drug resistance (8).

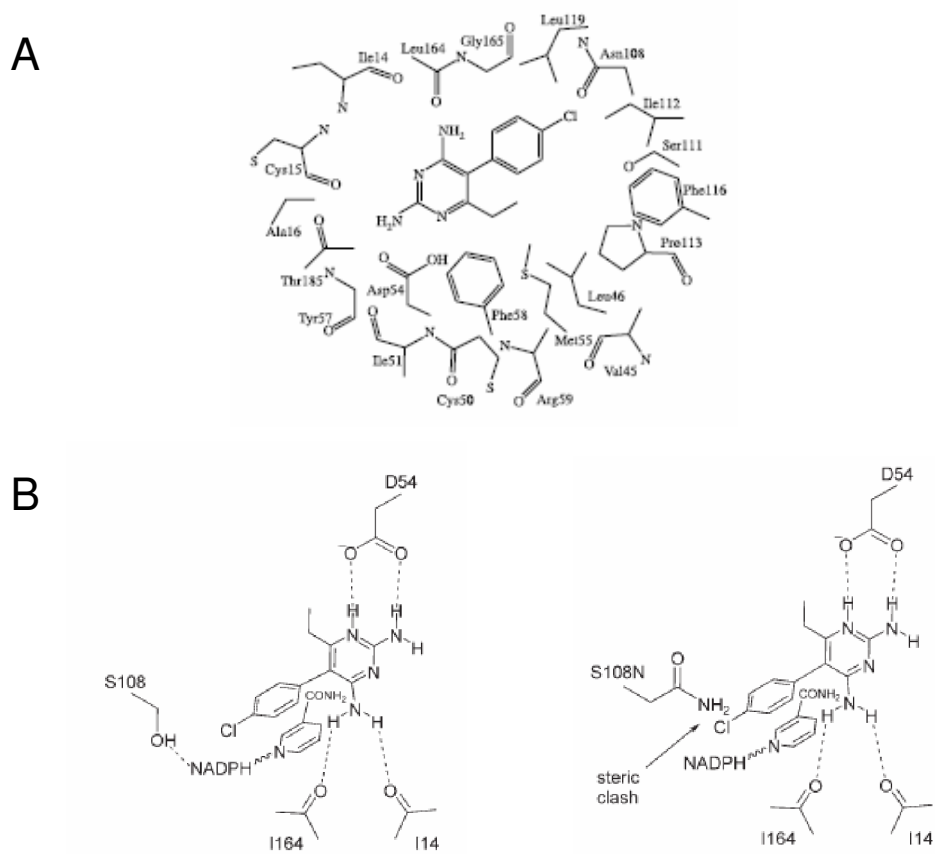


Figure 1.4 Pyrimethamine-inhibitor interactions at the active site of the DHFR enzyme with the mutations associated with resistance. (A) Mutations at codons 51I, 59R, 108N, and 164L cause steric hindrance that prevents binding of the inhibitor to the active site. (B) Amino acid change from serine (left) to asparagine (right) at codon 108 creates a steric clash that reduces the ability of pyrimethamine to bind to the active site. *Figures adapted from (A) Maitarad et al. (2009) and (B) Schlitzer (2007).*

Similarly, resistance to sulfadoxine has been associated with mutations at codons 436, 437, 540, 581, and 613 in the *dhps* gene. Sulfadoxine, a competitive antagonist of *p*-aminobenzoic acid, inhibits the synthesis of DHF. The SNPs effectively reduce the binding affinity of the inhibitor, thus allowing the parasite to utilize the folate pathway to synthesize nucleotides and amino acids (Figure 1.5) (42, 70).

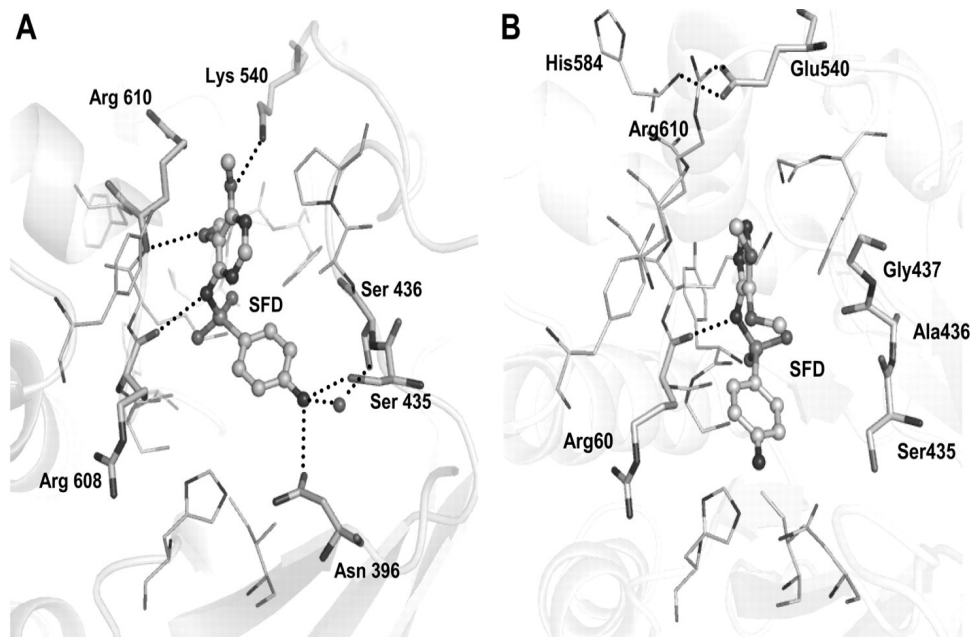


Figure 1.5 Sulfadoxine-inhibitor interactions at the active site of the DHPS enzyme with the mutations associated with resistance. (A) There are 5 direct hydrogen-bond interactions between the inhibitor and the wild-type amino acid residues. (B) Amino acid changes at codons 436, 437, and 540 induce conformational changes that reduce the number interactions between the inhibitor and the binding pocket. SFD = sulfadoxine. *Figure adapted from Lumb et al. (2009).*

Multiple *in vitro* and *in vivo* studies have shown an association between SP treatment failure and SNPs within the *dhfr* and *dhps* genes. The discovery of the polymorphisms conferring resistance against SP stemmed from enzymatic

assays by Cowman *et al.* (1988, 1994, 1997). Through expression and purification of the *pfdhfr* and *pfdhps* genes, this group analyzed the impact of SP on enzyme activity. Sequencing of the genes enabled the researchers to identify the alleles linked to either sulfadoxine or pyrimethamine resistance. Isolates with the identified alleles showed reduced enzymatic activity compared against the strains with the wild-type genotype.

Resistance to SP is multigenic and the accumulation of SNPs culminates in decreased sensitivity. The triple mutations (S108N/N51I/C59R) and double mutations (S436F and A613S/T) in *pfdhfr* and *pfdhps* genes, respectively, display increased resistance both *in vitro* and *in vivo* (39). Kublin *et al.* (2002) have shown that the simultaneous presence of SNPs at *pfdhfr* codon 59 and *pfdhps* codon 540 are useful predictors for a quintuple mutant (39). However, the accumulated SNPs have varying levels of resistance, whereby *in vivo* studies have shown relatively lower levels of resistance compared with *in vitro* studies. It is speculated that immunity plays a role in controlling the rise in parasitemia. As a result, many researchers feel that results from either type of study cannot be extrapolated to describe people who have impaired immune status, such as pregnant women (10). Thus, it is important to develop a surveillance program that monitors the genotypes associated with resistance among pregnant women.

### **1.3.3 Analysis of treatment failure**

The WHO has outlined a systematic protocol to carry out *in vivo* studies, which measures both antimalarial efficacy and parasitological resistance. The general description for therapeutic efficacy is the reduction in parasite biomass

with the concurrent decline of symptoms. Parasitological resistance does not take into account the signs or symptoms of clinical disease, but rather the concentration of the parasite within the human host. These two measurements are more appropriate indicators for high-levels of resistance and consequently will overestimate treatment failure (65). The 28-day follow-up assessment for drug efficacy provides insight towards *in vivo* pharmacodynamics, albeit potentially confounded by host factors.

Host biology and immune status play a role in drug efficacy that cannot be ignored. *In vivo* studies, which are primarily clinical trial studies, are the gold standard for measuring antimalarial drug efficacy; but they are also useful in assessing parasitological resistance. These studies allow researchers to characterize the relationship between immunity and treatment. There are fundamental gaps in the understanding of immune response and drug efficacy among pregnant women, in part due to the exclusion of pregnant participants in clinical trials. Studies based on mathematical modeling have predicted increasing spread of resistance using an antimalarial that has a long elimination period and has existing mechanisms of resistance (56). Immunity is also affected by the intensity of transmission (high versus low). People living in high transmission areas are more likely than those in low transmission areas to have acquired immunity against *P. falciparum*, which allows the person to resolve the infection (80)

*In vivo* testing still remains the best method for evidence-based policy decision-making (65). Results from *in vivo* studies may overestimate the true rate

of resistance due to confounding factors such as poor drug quality, inadequate dosing, and non-compliance (65, 69). The feasibility of performing *in vivo* testing in high transmission areas is limited by high costs and substantial time requirements.

The limited reliability and capacity to perform *in vivo* testing for surveillance has prompted researchers to move toward inexpensive techniques such as *in vitro* testing to measure drug resistance. *In vitro* testing (also known as *ex vivo*) entails culturing the parasites obtained from a patient and testing the culture against the drug to determine the half maximal inhibitory concentration, or IC50. *In vitro* testing allows researchers to measure the intrinsic sensitivity of the parasite to the drug. One of the limitations associated with *in vitro* testing is to obtain venous blood that is rich in parasites. A limitation to this method is the exclusion of host-related factors, which potentially alter the pharmacokinetics of the drug.

An advantage of *in vitro* testing is its ability to detect changes in susceptibility during the early stages of infection. Despite advances, the applicability of these *in vitro* tests is limited by their poor reflection of clinical outcome and in turn an inability to provide substantial proof for changing drug policy. A further disadvantage of this methodology is the inability to continuously culture *Plasmodium* species other than *P. falciparum*. As a result of this, researchers cannot measure the impact of antimalarials against the other infecting *Plasmodium spp.*

### **1.3.4 Need for surveillance of SP-resistance**

Current reviews on SP use for IPTp suggest that an alternative drug should be used for chemoprophylaxis. Although randomized control trials on SP-IPTp are exhibiting failure rates as high as 58%, there are no guidelines in place to direct national policies to halt the use of SP for IPTp in the face of resistance. As mentioned, treatment failure does not equate with parasitological resistance, thereby reinforcing the need to develop surveillance tools to measure the impact of antimalarial resistance on failing IPTp programs.

## **1.4 Methods of molecular surveillance for SP**

### **1.4.1 Monitoring of parasite drug resistance**

Since 2001, the WHO has implemented several strategies for monitoring drug-resistant parasites, including *in vivo* therapeutic efficacy tests, *in vitro* susceptibility testing, and use of molecular markers to identify the presence of mutations associated with reduced sensitivity to SP. Therapeutic efficacy tests are considered reflections of clinical situations; test results are classified as adequate clinical response, early treatment failure, late clinical failure or late parasitological failure. Identification of the parasite molecular markers linked with treatment outcome has improved the capacity to both monitor any emerging resistance and predict treatment failure (64). Risk to SP treatment failure has been shown to increase when the number of mutations within *dhfr* and *dhps* gene increases (64).

### **1.4.2 Molecular tests**

Nucleic acid amplification assays, such as the Polymerase Chain Reaction (PCR), have greatly improved the sensitivity and specificity for detecting drug

resistance. Performed on a thermal cycler, the reaction consists of alternate cycles of heating and cooling to allow the *Taq* polymerase enzyme to amplify specific target sequences within the parasite genome (amplicons). PCR assays have improved malarial diagnostic capabilities through improved differentiation between recrudescence infections from re-infections, detection of polyclonal infections, and differentiation of infecting species. Most national surveillance programs utilize a restriction fragment length polymorphism (RFLP) technique to detect the mutations within the *dhfr* and *dhps* genes. This particular method entails a nested-PCR followed by a restriction enzyme digest. Gel electrophoresis is performed to visualize the resulting banding pattern from the digest. RFLP is time-consuming, laborious, and prone to contamination from intermediary steps. DNA sequencing is another method for genotyping; however, much like RFLP, throughput is limited by its lengthy process and multiple steps. Both RFLP and DNA sequencing are methods that cannot be easily automated and/or used for field-testing.

#### **1.4.2.1 Real-time PCR technology**

In the field of molecular diagnostics, real-time PCR technology has improved the capacity to quantify nucleic acids. Real-time PCR is also known as quantitative PCR because amplified products can be detected as the reaction progresses. Real-time PCR allows for the measurement of nucleic acid during the exponential phase (or log phase), in contrast to conventional PCR which measures amplified product at the end-point when the reaction is no longer exponential. Detection at each amplification cycle is achieved by including a fluorescent agent



in the reaction. Real-time PCR has proven to be invaluable for analysis of gene expression, detection of infectious agents, and genotyping of SNPs (36). With respect to SNP genotyping, there are a number of methods by which researchers are able to identify genetic polymorphisms. These methods often employ fluorescent resonance energy transfer (FRET) or detection systems such as hybridization probe assays, molecular beacons, and TaqMan® assays. FRET is simple by design and allows for the entire reaction to take place within a single vessel. The limitation, however, is the associated cost of employing fluorescently labeled oligonucleotides. With SNP analysis, a minimum of two probes per SNP, which can make the assay for multiple genotypes increasingly expensive.

#### **1.4.2.2 TaqMan® minor groove binding probes**

Alker *et al.* (2004) described one of the first *P. falciparum* genotyping assays that employed a real-time PCR platform. This particular assay used TaqMan® minor groove binding (MGB) probes to rapidly detect the SNPs in the *dhfr* and *dhps* genes associated with SP resistance. In this assay, both PCR and allelic discrimination are done simultaneously within the same step. MGB probes are designed to have a reporter and quencher dye covalently attached to the 5'- and 3'- end, respectively. Each reaction includes 2 probes; one for each allele and each probe has a different fluorophore attached. At the end of amplification, any fluorescence emitted will be generated by either the wild-type or mutant probe that has hybridized to the amplicon. This form of end-point detection is simple and sensitive.

### **1.4.2.3 Intercalating DNA-binding dyes**

An alternative to using PCR/FRET-based methods is to employ DNA binding dyes and exploit the differential melting properties of the amplicon at increasing temperatures. These dyes fluoresce only when bound to double-stranded DNA structures. After the PCR step, amplicons are subjected to a melting step, thereby causing DNA duplex structures to dissociate. This dissociation causes intercalating dyes to be released, and lose their fluorescence. There are weaker hydrogen bonds formed with mutant alleles, which causes duplex dissociation to occur at lower temperatures. This high resolution melting (HRM) allows wild-type alleles to be distinguished from mutant alleles. HRM was shown to be successful for mutation detection in cancer screening, detecting infectious agents, and for SNPs associated with *P. falciparum* resistance (5). Andriantsoanirina *et al.* (2009) were the first to describe a method that allowed nucleic acid sequences to be genotyped using HRM for malaria. Although the method described was sensitive, there were limitations in detecting SNPs that were in close proximity along the DNA. Similarly, this method was not efficient for detection of polyclonal samples with mixed alleles.

### **1.4.3 High-throughput genotyping using asymmetric PCR and MCA**

Molecular assays that are capable of surveying the predominant SNPs associated with SP resistance are recommended for regional research centers in Africa (39). In 2007, Montgomery *et al.* described a method that allowed high throughput genotyping for SNPs using asymmetric PCR and melting-curve analysis (MCA) within a closed system (51). This seamless method takes place

within a single tube containing an excess of the reverse primer and unlabeled probe; the limiting forward primer, DNA binding dye, and PCR reagents. Contamination is prevented in this closed system because handling of post-amplified products is not required. The principle objectives of the method were applied to genotype the SNPs associated with SP resistance in the *pfdhfr* and *pfdhps* genes.

For each SNP, the asymmetric PCR will produce an excess of the anti-sense strand. During the cooling stage of the MCA, the unlabeled probe binds to the excess DNA strand. When the MCA is heating to denaturing temperatures, the probe will dissociate from the template thereby causing the DNA binding dye to release and stop emitting fluorescence. The probe is designed to bind to the complementary wild-type sequence; however it can bind to the mutant sequence with lower affinity. DNA sequences with mutations will cause the probe to dissociate at a lower melting temperature compared to wild-type sequences (Figure 1.6). The software on the LightCycler® platform is able to determine this melting temperature and genotype the sample based on the melting properties.

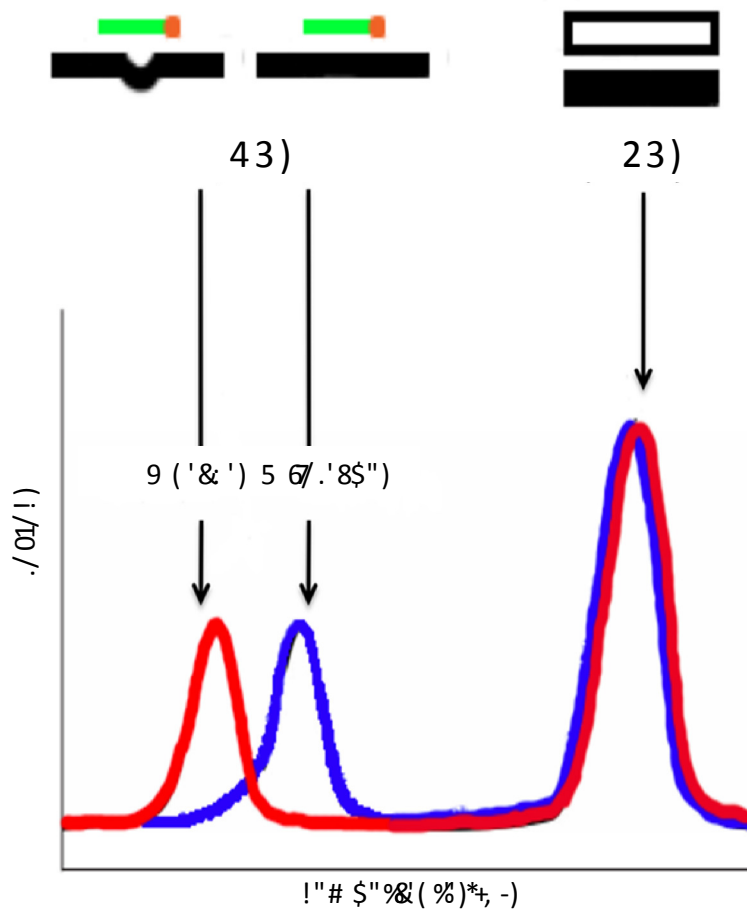


Figure 1.6 Melting peak profiles for wild-type and mutant sequences. The peak at the higher temperature corresponds to melting of the full-length amplicon duplex (AD) whereas the lower temperature peaks correspond to the melting of the genotyping probe (GD) from the amplicon. *Figure adapted from Montgomery et al. (2007).*

The method described is successful at genotyping the SNPs associated with SP resistance in the *pfdhfr* and *pfdhps* genes, particularly resolving the limitations described by Andriantsoanirina *et al.* (2009). However, a limitation to using real-time PCR platforms to genotype parasitic diseases is the fact that there is a huge infrastructure requirement to support its use. The LightCycler®, much

like all other real-time PCR platforms, is a fairly large instrument commonly used in reference laboratories. Many developing countries are not able to support the requirements for consistent power and high costs. As a result, the LightCycler® platform cannot be used in the field for genotyping *P. falciparum*, particularly for the areas that are in need of surveillance.

#### **1.4.4 Application onto a “nano” device**

There is poor transference of molecular research tests from developed countries to the developing countries in need of tools for surveillance. Developments in nano/microfluidic technologies are attempting to integrate assays onto portable devices that can potentially be used in the field (41). In 2010, Atrazhev *et al.* described the ability to perform PCR assays within photopolymerized polyacrylamide gel posts (6). In-gel PCR is performed on a prototype PCR platform, known as the Viriloc. The genotyping assay that was developed on the LightCycler can potentially be applied towards this in-gel technology. The implication of this application can lead to improvements in point-of-care testing for malaria in field sites.

#### **1.5 Hypothesis**

SNPs associated with malaria drug resistance are difficult to test in low resource settings due to the cost of equipment, energy requirements, and complicated assays. We hypothesize that samples can be genotyped for the codons associated with SP resistance based on the differences in melting properties between mutant and wild-type DNA sequences. This thesis aims to

develop a genotyping method for SNPs associated with SP resistance for potential use in low resource settings.

### **1.5.1 Objectives/research question**

To apply the SNP detection methods developed on the LightCycler onto the in-gel technology in order to genotype *P. falciparum* for mutations associated with SP resistance.

### **1.5.2 Study aims**

1. Develop an assay to genotype the SNPs in the *pfdhfr* and *pfdhps* genes associated with SP resistance based on the method described by Montgomery *et al.* (2007).
2. Validate the performance characteristics of this assay using reference and clinical samples.
3. Apply the genotyping method from the LightCycler to in-gel technology.

## Chapter 2<sup>1</sup> LightCycler® assay

### 2.1 INTRODUCTION

Sulfadoxine-pyrimethamine (SP) is widely used throughout sub-Saharan Africa for treatment of uncomplicated *P. falciparum* malaria and as Intermittent Preventive Therapy in pregnancy (47, 83). However, the efficacy of SP has been severely compromised by the rapid emergence of resistant strains (88). Resistance can largely be attributed to single nucleotide polymorphisms (SNPs) within the *P. falciparum dhfr* and *dhps* genes that inhibit the activity of enzymes involved in folate biosynthesis (66, 78, 91). With resistance to pyrimethamine, specific *pfdhfr* mutations (N51I, C59R, S108N) are associated with increased levels of resistance *in vitro* and clinical treatment failure *in vivo* (8, 66). Accumulation of mutations at codons 51, 59, and 108 confers increasing levels of resistance, with the triple mutant becoming the dominant genotype in many endemic areas (88). Similarly, specific *pfdhps* polymorphisms (S436F, A437G, K540E, A581G, A613T) confer resistance against sulfadoxine (3, 66, 79). Recently, a mutation at *pfdhfr* codon 164 (I164L) has emerged as a new predictor of treatment failure and quadruple mutant genotypes have been identified in Southeast Asia, South America and Africa (47, 66). A mutation at *pfdhps* codon 540 in the presence of the mutation at *pfdhfr* codon 59 is valued as a strong predictor for treatment failure (49).

Methods that genetically identify SP-resistant genotypes underpin molecular

---

<sup>1</sup> A portion of this chapter has been published. Cruz, R., S. Shokoples, D. Manage, and S. K. Yanow. 2010. *Journal of Clinical Microbiology* 48 (9): 3081-3087.

surveillance efforts to monitor resistance. Many tools have been developed to genotype mutations within the *pfdhfr* and *pfdhps* genes, including techniques such as restriction fragment length polymorphism and nested PCR. Recently, the application of real-time PCR for genotyping malaria parasites has been described (85). Studies by Alker *et al.* (3, 4) used real-time PCR with sequence-specific probes to detect four of the *pfdhfr* and five of the *pfdhps* SNPs conferring resistance to SP. Despite excellent sensitivity reported for this assay, cross-reactivity between probes has been observed (57). Other methods include fluorescence resonance energy transfer (FRET) in conjunction with melt-curve analysis (MCA); hybridization probes are used to differentiate between wild-type and mutant sequences based on thermodynamic stability (5). However, these probes are added following the amplification step and increase the risk of nucleic acid contamination.

Recent advances in MCA have enabled detection of SNPs by high-resolution genotyping within closed-tube systems (5, 51). High-Resolution DNA Melting (HRM) analysis uses an intercalating dye that dissociates from double-stranded DNA at increased temperatures. The genotype is identified based on inherent differences in melting temperatures between wild-type and mutant DNA amplicons (5, 51). An alternative approach uses asymmetric PCR in the presence of the DNA intercalating dye LCGreen® Plus with an unlabeled probe specific to the SNP of interest (51). During asymmetric PCR, the sense strand of the amplicon is generated in excess, allowing the probe to anneal and form a duplex; LCGreen® Plus binds to the duplex, generating a fluorescent signal. During melt-



curve analysis, the probe dissociates from the amplicon resulting in a decrease in the fluorescent signal. If there is a base-pair mismatch between the probe and the amplicon, the probe will dissociate from the DNA template at a lower temperature compared to a perfectly matched sequence. Resolution of different SNPs is achieved by analyzing the melt-curve profiles for the probe-amplicon complex. Implementation of this assay has been reported for detection of polymorphisms and mutations associated with a number of human diseases including diabetes and cancer (24, 29). This method was applied to genotype polymorphisms in the *pfdhfr* and *pfdhps* genes from clinical specimens collected from travelers and immigrants with *P. falciparum* malaria in Alberta, Canada. This method demonstrated superior sensitivity to probe-based real-time PCR and offers a novel molecular tool for high-throughput genotyping of malaria.

## **2.2 MATERIALS AND METHODS**

**2.2.1 Plasmids.** A 641 bp region of the *dhfr* gene containing all four SNPs was amplified from *P. falciparum* 3D7 and V1/S genomic DNA using the following primers: forward, 5'-ATGATGGAACAAGTCTGCGA-3' and reverse, 5'-ACTAGTATATACATCGCTAACAGA-3'. Similarly, A 655 bp region of the *dhps* gene containing all five SNPs was amplified from *P. falciparum* HB3, 3D7, V1/S, and K1 genomic DNA and plasmid pPeru using the following primers: forward, 5'-TGAAATGATAAATGAAGGTGCTAGTGT-3' and reverse, 5'-AATTGTGTGATTTGTCCACAA-3'. DNA amplification of the *pfdhfr* gene was performed using a 2720 Thermal Cycler (Applied Biosystems) with the following

program: hold at 95°C for 5 min, 40 cycles of 95°C for 30 s, 55°C for 30 s, 72°C for 45 s. The annealing temperature for the amplification of the *pfdhps* gene was 48 °C. The amplicons were cloned into the vector pCR 2.1-TOPO using the TopoTA Cloning kit (Invitrogen). Clones were verified by sequencing. Plasmids were quantified by spectrophotometry and serially diluted from 10<sup>6</sup> copies to 10<sup>0</sup> to generate a standard curve.

**2.2.2 Control genomic DNA and clinical samples.** Genomic DNA from four strains of *P. falciparum* (3D7, 7G8, HB3, K1, W2, and V1/S) was obtained from the Malaria Reagent Repository Resource (<http://mr4.org>). Table 2.1 outlines the genotypes for the genomic DNA and plasmid used for generating the standard controls. DNA was serially diluted ten-fold from 1 µg/µL to 0.1 pg/µL in order to generate standards for melt-curve analysis. The laboratory strain 3D7 was cultured in human erythrocytes as described previously (89). Parasitemia was determined from Giemsa-stained thin smears and the number of parasites/µL of blood was calculated based on the parasitemia, an estimated concentration of 5x10<sup>9</sup> RBC/mL blood and a hematocrit of 3%. DNA was extracted using the Precision System Science (PSS) DNA Magtration System 12GC, following the DNA 200 extraction protocol (kit E2003) and eluted into a 100 µL volume (73). Clinical samples from patients infected with *P. falciparum* were obtained from the Provincial Laboratory for Public Health in Edmonton, Alberta, Canada. DNA was extracted from 40 µL of whole blood according to the protocol described above. This study was approved by the Health Research Ethics Board of the University of Alberta.

Table 2.1 *Dhfr* and *dhps* haplotypes for *P. falciparum* strains and plasmid

ISOLATE	<i>pf dhfr</i> codon				<i>pf dhps</i> codon				
	51	59	108	164	436	437	540	581	613
Wild-type <sup>a</sup>	N	C	S	I	S	A	K	A	A
Mutant <sup>b</sup>	I	R	N	L	F	G	E	G	S/T
3D7	N	C	S	I	S	G	K	A	A
V1/S	I	R	N	L	F	G	K	A	T
HB3	N	C	N	I	S	A	K	A	A
K1	N	R	N	I	S	G	K	G	A
W2	I	R	N	I	F	G	K	A	S
pPeru <sup>c</sup>	n/a	n/a	n/a	n/a	S	G	E	G	A

<sup>a</sup> Wild-type amino acid sequences for codons in the *pf dhfr* and *pf dhps* genes

<sup>b</sup> Mutant amino acid sequences for codons in the *pf dhfr* and *pf dhps* genes

<sup>c</sup> pPeru is a plasmid containing the entire *pf dhps* gene and not the *pf dhfr* gene (depicted as not available, n/a)

**2.2.3 Real-time PCR and melt-curve analysis.** Asymmetric PCR was carried out based on the methodology described previously (51) using the LightCycler® 2.0 (Roche) with conditions optimized for amplification and detection of the SNP targets from the *pf dhfr* and *pf dhps* genes. Primers and unlabeled probes were synthesized by IDT (Iowa, USA) and are listed in Table 2.2. Probes are complementary to the wild-type sequence and modified at the 3' end with a C3-spacer (51). For codons in both *pf dhfr* and *pf dhps* genes, the total reaction volume of 20 µL consisted of 2 µL of DNA, 1x PCR buffer (Promega), 1x LC Green® Plus (Idaho Technology Inc., USA), 50 nM of forward primer, 500 nM each of reverse primer and unlabelled probe, 200 µM of dNTPs, 3.5 mM of MgCl<sub>2</sub>, 0.032% BSA, and 4.0 U of Taq (Promega). The amplification program consisted of an initial denaturation at 95 °C for 2 min, 40 cycles of 95 °C for 30 s,

48 °C for 10 s, and 72 °C for 30 s, followed by 10 minutes at 72°C. The ramp rates for the denaturation, annealing, and extension segments of the PCR were 20 °C/s, 3 °C/s, and 0.1 °C/s, respectively. Melt-curve analysis for all SNPs was performed as follows: 95 °C for 30 s, 55 °C for 1 min, with a ramp rate of 0.1 °C/s and final denaturation at 95 °C for 30 s. The software program for the LightCycler® (version 4.1) was used to genotype samples according to the melt-curve profiles. Control genomic DNAs were used as external standards to genotype the panel of clinical samples. To generate mixtures of wild-type and mutant DNA, gDNA (1 ng/μL) from clinical samples of each genotype were mixed at 1:1, 1:3 and 3:1 ratios in the PCR-MCA reaction.

Table 2.2 Primer and probe sequences for the SNPs in the *pfdhfr* and *pfdhps* genes

TARGET	SEQUENCE
DHFR-51	F: 5'-TGA GGT TTT TAA TAA CTA CAC ATT TAG AGG TCT-3' <sup>a</sup> R: 5'-TAT CAT TTA CAT TAT CCA CAG TTT CTT TGT TT-3' <sup>a</sup> P: 5'-ACC ATG GAA ATG TAA TTC CCT AGA TAT GA-C3spacer
DHFR-59	F: 5'-TGA GGT TTT TAA TAA CTA CAC ATT TAG AGG TCT-3' <sup>a</sup> R: 5'-TAT CAT TTA CAT TAT CCA CAG TTT CTT TGT TT-3' <sup>a</sup> P: 5'-ATA TGA AAT ATT TTT GTG CAG TTA CAA CA-C3spacer
DHFR-108	F: 5'-TGG ATA ATG TAA ATG ATA TGC CTA ATT CTA A-3' <sup>a</sup> R: 5'-AAT CTT CTT TTT TTA AGG TTC TAG ACA ATA TAA CA-3' <sup>a</sup> P: 5'-TAG TTA TGG GAA GAA CAA GCT GGG AAG C-C3spacer
DHFR-164	F: 5'-ATC ATT AAC AAA GTT GAA GAT CTA ATA GTT TTA C-3' <sup>b</sup> R: 5'-TCG CTA ACA GAA ATA ATT TGA TAC TCA T-3' <sup>b</sup> P: 5'-ATA AAT GTT TTA TTA TAG GAG GTT CCG TT-C3spacer
DHPS-436/437	F: 5'-TGA AAT GAT AAA TGA AGG TGC TAG TGT-3' <sup>a</sup> R: 5'-AAT ACA GGT ACT ACT AAA TCT CTT TCA CTA ATT TTT-3' <sup>a</sup> P: 5'-GTG GAG AAT CCT CTG CTC CTT TTG TTA TAC C-C3spacer
DHPS-540	F: 5'-TGT AGT TCT AAT GCA TAA AAG AGG-3' R: 5'-CCA ATA TCA AAT AGT ATC CTA TAA CGA-3' P: 5'-CCA CAT ACA ATG GAT AAA CTA ACA AAT TAT GAT AAT-C3spacer
DHPS-581	F: 5'-GTA TTA AAT GGA ATA CCT CGT TAT AGG-3' R: 5'-TTG AAT ATC CAA TAA AAA GTG GAT ACT-3' P: 5'-GGA TTA GGA TTT GCG AAG AAA CAT GAT C-C3spacer
DHPS-613	F: 5'-CTC TTA CAA AAT ATA CAT GTA TAT GAT GAG-3' R: 5'-AAT TGT GTG ATT TGT CCA CAA-3' P: 5'-GAA AAA GAT TTA TTG CCC ATT GCA TGA ATG-C3spacer

F: forward primer, R: reverse primer, P: probe

<sup>a</sup> Alker et al, 2004

<sup>b</sup> Alker et al, 2005

**2.2.4 Pyrosequencing and direct sequencing.** Pyrosequencing was used to confirm the genotype at codons 51, 59, and 108, essentially as described by Zhou *et al.* (92) with modifications to the primers (Table 2.3) and conditions. Nested PCR was performed in 25  $\mu$ L (first round) or 100  $\mu$ L (second round) reactions with 1x PCR buffer (Promega), 100  $\mu$ M dNTPs, 1.5 mM MgCl<sub>2</sub>, 200 nM primers,

and 0.025 U/ $\mu$ L Taq (Promega). First round PCR: 95°C for 5 min; 25 cycles of 94°C for 30 s, 55°C for 30 s, 68°C for 45 s; 10 cycles of 94°C for 30 s, 52°C for 30 s, 68°C for 45 s. For nested reactions, 10  $\mu$ L from the first round served as template. Second round PCR: 95°C for 5 min; 15 cycles of 94°C for 30 s, 55°C for 30 s, 68°C for 45 s; 20 cycles of 94°C for 30 s, 52°C for 30 s, 68°C for 45 s; 10 cycles 94°C for 30 s, 50°C for 30 s, 68°C for 45 s. Pyrosequencing reactions were carried out on the PSQ™ 96MA with the nucleotide dispensation order 10(GATC). For the clinical samples, SNP genotyping by pyrosequencing was carried out by Sandra Shokoples. For codon 164 in the *pfdhfr* gene, purified PCR products (212 bp) were sequenced in both directions (Applied Genomics Centre, University of Alberta) using the amplification primers (Table 2.2). Similarly, for all the codons in the *pfdhps* gene, purified PCR products were sequenced in both directions (Cross Cancer Institute, University of Alberta) using the amplification primers (Table 2.2).

Table 2.3 Pyrosequencing primers

Primer name	Sequence (5'-3')	Final concn (nM)	Reaction
pfdhfr-F1	ATGATGGAACAAGTCTGCGAC <sup>a</sup>	200	First-round PCR for codons 51, 59, 108; second-round PCR for codons 51, 59
pfdhfr-R1	TACATCACATTCATATGTAC	200	First-round PCR for 51, 59, 108
pfdhfr-F2	CCCTAGATATGAAATATTTT	200	Second-round PCR for 108
pfdhfr-R2	Biotin-TGTTCTTCCCATAACTACAAC	200	Second-round PCR for 51, 59
pfdhfr-R3	Biotin-CACATTCATATGTAATATTT	200	Second-round PCR for 108
51F	GGTCTAGGAAATAAAGGAGT <sup>a</sup>	500	Pyrosequencing
59F	CCCTAGATATGAAATATTTT <sup>a</sup>	500	Pyrosequencing
108	GTTGTAGTTATGGGAAGAACA	500	Pyrosequencing

<sup>a</sup> Zhou *et al.*, 2006

**2.2.5 Taqman PCR.** The Taqman-based real-time PCR method described by Alker *et al.* (3, 4) was performed on the ABI Prism 7000 sequence detection system using published primers (IDT, USA) and probes (Applied Biosystems, USA) for the SNPs in the *pfdhfr* gene (3, 4).

**2.2.6 Statistical analysis.** McNemar's test was used to test the null hypothesis that the accuracy of genotyping the clinical samples against the "gold standard" using the TaqMan method is equal to the accuracy of genotyping the same samples using the LightCycler® method for the SNPs in the *pfdhfr* gene.

## 2.3 RESULTS

### 2.3.1 Sensitivity of melt-curve analysis for genotyping *pfdhfr*

A method for high-resolution melt-curve analysis (MCA) was developed to genotype four SNPs within the *pfdhfr* gene that are associated with resistance to

the antimalarial pyrimethamine. For each SNP, asymmetric amplification of the target region within *pfdhfr* was optimized to generate an excess of the sense strand. As described by Montgomery *et al.* (51), reactions include an antisense oligonucleotide probe that recognizes the SNP of interest and binds to the excess sense DNA produced by asymmetric PCR. During MCA, the dissociation of the probe from the template occurs at a specific melting temperature ( $T_m$ ) and results in a reduction in fluorescence as the duplex DNA strands separate. In this study, probes were designed to complement the wild-type SNP; thus, the dissociation of the probe occurs at a lower temperature when there is a mismatch between the probe and template.

Genomic DNA extracted from *P. falciparum* 3D7 and V1/S strains was used to develop the melting standards for the wild-type and mutant sequences, respectively. The 3D7 strain contains the wild-type sequence at each target codon: N51, C59, S108 and I164, whereas the V1/S strain contains the mutant sequences: 51I, 59R, 108N and 164L. Representative melt curves from these two strains are shown for each of the four probes (Figure 2.1). The peak that melts at higher temperatures corresponds to the full-length amplicon from the PCR reaction while the peak that dissociates at lower temperatures corresponds to the melting of the probe-amplicon duplex. For all four SNPs, the wild-type and mutant genotypes were clearly distinguished based on their melt-curve profiles.



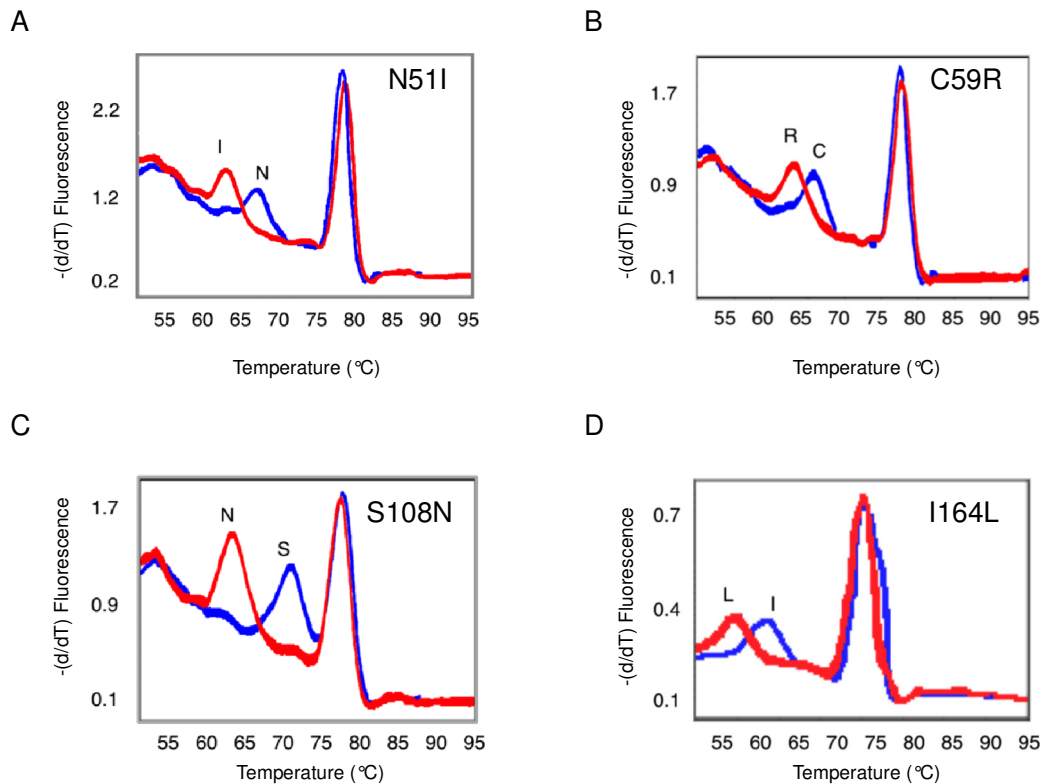


Figure 2.1 Genotyping of SNPs in the *pfdhfr* gene by asymmetric PCR and melt-curve analysis. Melting curves from isolates containing either the wild-type (blue) sequence or the mutant (red) sequence in the four codons: (A) N51I, (B) C59R, (C) S108N, and (D) I164L.

Serial dilutions of plasmids containing the amplified region of the *pfdhfr* gene were used to determine the analytical sensitivity of melt-curve analysis for genotyping at each SNP. The genotyping program on the LightCycler® identified the template as either wild-type or mutant based on a comparison with external genomic DNA standards. Reactions were performed in triplicate to determine the reproducibility of the assay for correct identification of wild-type and mutant strains. For all of the SNPs, genotypes were consistently identified at 100 template copies (Table 2.4). Although PCR amplification occurred at lower plasmid dilutions, the shape of the melt curves was broader and genotypes were scored either as “negative” or “unknown” by the software program. A “negative”

sample lacks sufficient DNA template to generate a melt curve, whereas an “unknown” sample implies that the melt curve generated does not have a shape similar to that of the standards.

Table 2.4 Analytical sensitivity of the genotyping assay for each SNP in the *pfdhfr* gene using MCA

Plasmid	Copies	Detection at the codon <sup>a</sup>			
		51	59	108	164
Wild-type	10 <sup>3</sup>	3/3	3/3	3/3	3/3
	10 <sup>2</sup>	3/3	3/3	3/3	3/3
	10 <sup>1</sup>	1/3	1/3	0/3	1/3
	10 <sup>0</sup>	0/3	0/3	0/3	0/3
Mutant	10 <sup>3</sup>	3/3	3/3	3/3	3/3
	10 <sup>2</sup>	3/3	3/3	3/3	3/3
	10 <sup>1</sup>	0/3	0/3	3/3	0/3
	10 <sup>0</sup>	0/3	0/3	0/3	0/3

<sup>a</sup>Results are reported as number of replicates detected in triplicate reactions.

The sensitivity of the assay was further evaluated with genomic DNA extracted from *P. falciparum* strains containing either the wild-type or mutant sequences (Table 2.5). Concentrations of genomic DNA were tested between 1 µg/µL and 0.1 pg/µL. Correct identification of the genotype in triplicate reactions was achieved at template concentrations of 10 pg/µL or 1 pg/µL, depending on the specific SNP. Furthermore, mixtures of the gDNA from the wild-type and mutant templates were prepared to determine the sensitivity of the assay in detecting mixed infections (data not shown). Both the wild-type and mutant SNPs were detected in triplicate reactions when present at equal concentrations. At positions 51 and 108, the mutant could be detected in 3/3 reactions even at a 1:3 ratio with wild-type DNA. At positions 59 and 164, the mutant SNP was detected in 2/3 replicates when present at this lower ratio.

Table 2.5 Limit of detection for *pfdhfr* SNP identification by MCA

Codon	SNP	Strain <sup>a</sup>	gDNA concn <sup>b</sup> (pg/! L)
51	N	3D7	1
	I	7G8	1
59	C	3D7	1
	R	W2	1
108	S	3D7	1
	N	7G8	10
164	I	3D7	1
	L	V1/S	10

<sup>a</sup>*P. falciparum* laboratory strain

<sup>b</sup>Lowest concentration of gDNA detected in triplicate reactions

To determine the dynamic range of the assay, the parasite strain 3D7 was grown in culture to a parasitemia of approximately 20% and serially diluted with uninfected erythrocytes. A range of parasite concentrations from  $3 \times 10^4$  parasites/ $\mu$ L blood to 1.5 parasites/ $\mu$ L was tested. The 3D7 strain is wild-type at all four *dhfr* SNPs, enabling us to determine the limit of detection for the wild-type genotype. Genomic DNA was extracted from these samples and tested by MCA (Table 2.6). MCA was able to correctly identify the wild-type genotype from cultures diluted to 1500 parasites/ $\mu$ L for codon 59, 15 parasites/ $\mu$ L for codons 51 and 164, and 1.5 parasites/ $\mu$ L for codon 108.

Table 2.6 Dynamic range of genotyping assay for *pfdhfr* using serially diluted wild-type cultures

Parasites/! L blood	Detection at the codon <sup>a</sup>			
	51	59	108	164
3.0 x 10 <sup>4b</sup>	3/3	3/3	3/3	3/3
1.5 x 10 <sup>4</sup>	3/3	3/3	3/3	3/3
1.5 x 10 <sup>3</sup>	3/3	3/3	3/3	3/3
1.5 x 10 <sup>2</sup>	3/3	2/3	3/3	3/3
1.5 x 10 <sup>1</sup>	3/3	0/3	3/3	3/3
1.5	1/3	0/3	3/3	0/3

<sup>a</sup>Results are reported as number of replicates detected in triplicate reactions.

<sup>b</sup>*P.falciparum* 3D7 cultures at approximately 20%

### 2.3.2 Sensitivity of melt-curve analysis for genotyping *pfdhps*

Genomic DNA extracted from isolate HB3 was used as the wild-type control for all the SNPs in the *pfdhps* gene. Isolates K1 and pPeru were used as the mutant control for codons 581 and 540, respectively. Isolate V1/S was used as the mutant control for codons 436, 437, and 613. The 3D7 strain had a unique sequence that was wild-type for codon 436, but mutant at codon 437. Melt curves from the wild-type and mutant strains are shown for all four probes (Figure 2.2). The probe for the 436 SNP overlaps with the 437 SNP since these are adjacent codons. As a result, three probe-amplicon peaks are potentially generated based on the possible sequences: 1) wild-type for both codons (isolate HB3), 2) mutant for both codons (isolate V1/S), and 3) wild-type for one codon, but mutant for the other (isolate 3D7) (Figure 2.2, panel A).

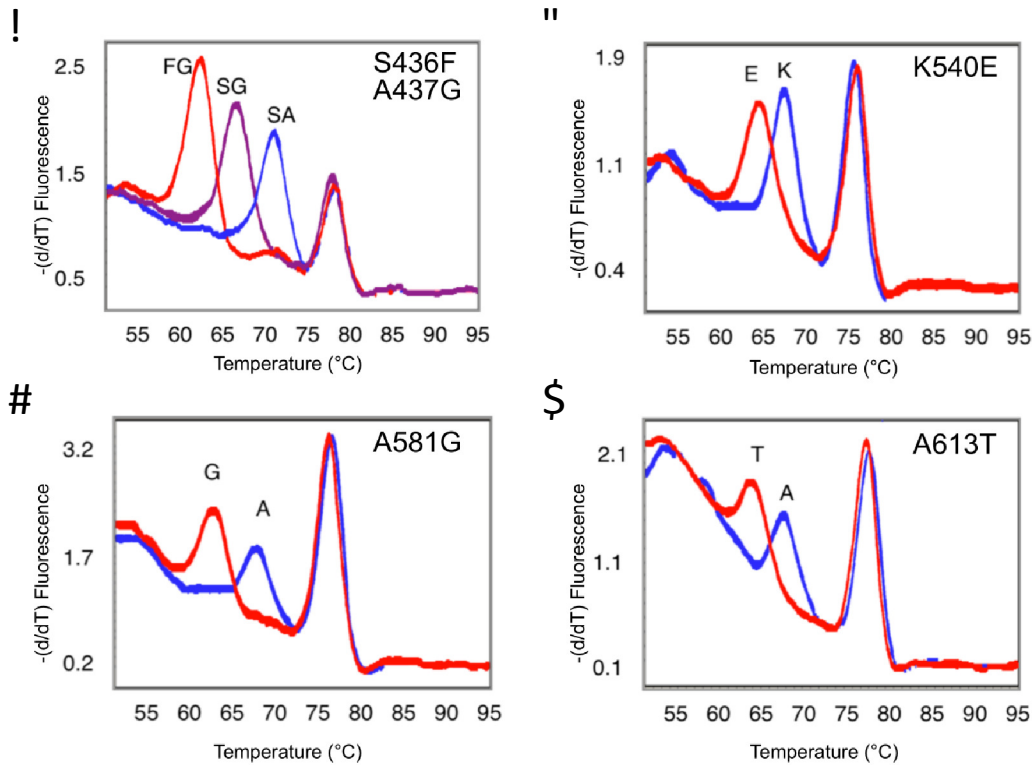


Figure 2.2 Genotyping of SNPs in the *pfdhps* gene by asymmetric PCR and melt-curve analysis. SNPs could be genotyped as either wild-type (blue) or mutant (red) for each SNP (A; codons 436 and 437, B; codon 540, C; codon 581, and D; codon 613). For codons 436 and 437, one melting curve is from an isolate bearing a mutant allele at either codon (panel A; purple curve).

To determine the analytical sensitivity of the melt curve assay, plasmids containing the amplified region of the *dhps* gene were serially diluted. Much like the *pfdhfr* gene, the LightCycler® distinguished the template as either wild-type or mutant based on a comparison with the external genomic DNA standards. Genotypes were consistently identified at a range of 10 to 100 template copies, depending on the specific SNP (Table 2.7). Genomic DNA extracted from the isolates that carried either the wild-type or mutant sequences were tested to further measure the sensitivity of the assay (Table 2.8). Correct identification of the genotype in triplicate reactions was achieved at template concentrations

ranging between 10 pg/μl and 0.1 pg/μl, depending on the specific SNP (Table 2.9).

Table 2.7 Analytical sensitivity of the genotyping assay for each SNP in the *pfdhps* gene using MCA

C,)	* #%	! " +1 (%	A-.- /. 1' \$% %B- %" #"\$' %			
%	%	%	678967: %	=6; %	=>@%	8@7%
%	%	%	%	%	%	%
[ 1#\ 3+- %	@ 7%	797%	797%	797%	797%	797%
%	@ <%	797%	797%	797%	797%	797%
%	@ @%	797%	797%	797%	; 97%	797%
%	@ ; %	@7%	; 97%	; 97%	; 97%	; 97%
%	%	%	%	%	%	%
%	%	%	%	%	%	%
] H)\$. %	@ 7%	797%	797%	797%	797%	797%
%	@ <%	@7%	797%	; 97%	; 97%	797%
%	@ @%	; 97%	; 97%	; 97%	; 97%	797%
%	@ ; %	; 97%	; 97%	; 97%	; 97%	; 97%
%	%	%	%	%	%	%

\*G- (H. (%5- % + " 5.- #%( %H\* E- 5%1% +, 1/). - (%6-.- /.- #%\$%51+, 1/). - % ) / . 1' \$(%

Table 2.8 Limit of detection for *pfdhps* SNP identification by MCA

!"#\$%	0&C%	0.5) \$" %	J A&K% \$/\$#% L+J 9% M%
%	%	%	%
678967: %	OK%	NO7%	@%
%	OP%	7A: %	; '@%
%	QP%	R@0%	@%
%	%	%	%
=6; %	S %	NO7%	@%
%	T%	\$%!	\$%!
%	%	%	%
=>@%	K%	NO7%	@%
%	P%	S @%	@%
%	%	%	%
8@7%	K%	NO7%	@%
%	U%	R@0%	@ %
%	%	%	%

"G- (H. (%5- % + " 5- #%( %H\* E- 5%l% +, 1/). - (%- .- /.- #0% \$%5+ , 1/). - % ) / . 1' \$ (%  
 #V" W- (. %" \$ /- \$ . 5). 1' \$ %l% A&K% - .- /.- #0% \$%5+ , 1/). - % ) / . 1' \$ (%  
 \$% X% " . %2) 1) E, - %

Table 2.9 Dynamic range of genotyping assay for SNPs in the *dhps* gene using a serially diluted *P. falciparum* strain 3D7

C) 5) (1- (9D, %	A- .- / . 1' \$ % %B- %" # " \$ " %			
E, " " #%	678967: %	=6; %	=>@%	8@7%
%	%	%	%	%
7'; %6 6#%	797%	797%	797%	797%
@=70@ 60%	797%	797%	797%	797%
@=70@ 70%	797%	797%	797%	797%
@=70@ <0%	797%	797%	797%	@7%
@=70@ @%	797%	; 97%	797%	797%
@=0%	; 97%	; 97%	; 97%	; 97%
%	%	%	%	%

"G- (H. (%5- % + " 5- #%( %H\* E- 5%l% +, 1/). - (%- .- /.- #0% \$%5+ , 1/). - % ) / . 1' \$ (%

Prepared mixtures of the gDNA with both the wild-type and mutant sequences for the SNPs in the *pfdhps* gene were tested to determine the sensitivity

of the assay in detecting polyclonal infections. Genomic DNA carrying the mutation sequence at codon 540 was unavailable and thus sensitivity for mixed infections could not be measured for this SNP. Compared to the “mixed infection” reactions for the SNPs in the *pfdhfr* gene, the codons in the *pfdhps* gene do not have the same capacity to detect both the wild-type and mutant SNPs when equal concentrations are present. At positions 581 and 613, the mutant could be detected in 3/3 reactions even at a 1:3 ratio with the wild-type DNA. For codons 436/437, the mutant sequence could be detected at a 1:3 ratio with the wild-type especially if the template has mutations at both codons (V1/S strain). If there were both the wild-type and mutant sequences at the 436/437 codons (3D7 strain), then the calling was “wild-type.” Genotyping for these two SNPs had to be confirmed manually.

### **2.3.3 Evaluation of MCA with clinical samples**

*Pfdhfr*: To evaluate the performance of the assay with clinical samples, a panel of 44 blood samples was genotyped at all four SNPs of the *pfdhfr* gene by MCA. All specimens were confirmed *P. falciparum* infections as determined by real-time PCR performed in a clinical diagnostics laboratory (73). Genotypes were identified by the LightCycler® software at all four SNPs in 30 of the 44 samples. The sensitivity of the assay to genotype a given SNP was calculated based on the number of specimens tested that were assigned a genotype by the LightCycler® software. For the panel of samples, the sensitivity of genotype calling for each individual SNP was the following: 93.2% at codon 51, 86.4% at codon 59, 84.1% at codon 108, and 81.8% at codon 164 (Table 2.10). To determine the accuracy of



the genotype assigned by MCA, the identification of each SNP was compared to a gold standard. Pyrosequencing served as the gold standard for codons 51, 59 and 108. In 2/44 samples, the genotype could not be identified at positions 51 and 108 by pyrosequencing and these were genotyped by direct sequencing. Direct sequencing also identified the genotype of all 44 samples at codon 164 and served as the gold standard for this SNP. There were no samples that could be identified by MCA but not by either of the sequencing methods. Concordance between MCA and sequence-based methods for the correct identification of the genotype ranged from 84% to 100% (Table 2.10). In the 30 samples for which a genotype was called at all 4 SNPs by MCA, 24 (80%) had the correct genotype. Of the specimens that could not be genotyped, or called “negatives”, 12/14 had a parasitemia less than 0.1% by microscopy (data not shown). This establishes the clinical sensitivity for the assay where the level of infection is below the limit of detection.

The McNemar’s test revealed that for codon 51 in the *pfdhfr* gene, the accuracy of the TaqMan assay is not significantly different from the accuracy of the LightCycler® assay ( $p = 0.2207$ ). However, for codons 59, 108, and 164, the McNemar’s test indicated that there was a statistically significant difference ( $p < 0.001$ ) between the accuracy of genotyping by the TaqMan assay and the accuracy of genotyping by MCA (Table 2.10).

Table 2.10 Concordance between the MCA and TaqMan assays for the SNPs in the *pfdhfr* gene compared against the gold standard

Codon	No. samples	MCA			TaqMan		
		No. genotyped	Sensitivity <sup>a</sup> (CI95%)	Concordance <sup>b</sup> (CI95%)	No. genotyped	Sensitivity <sup>a</sup> (CI95%)	Concordance <sup>b</sup> (CI95%)
51	44	40	93.2% (79-96%)	97.5% (87-100%)	37	84.1% (71-92%)	97.3% (85-99%)
59*	44	38	86.4% (72-94%)	84.2% (73-94%)	39	88.6% (76-95%)	25.6% (15-41%)
108*	44	37	84.1% (71-92%)	94.6% (82-99%)	4	9.1% (4-21%)	25% (4-70%)
164*	44	36	81.8% (68-90%)	100% (91-100%)	18	40.9% (28-56%)	100% (82%-99)

<sup>a</sup> Percent of total specimens that were genotyped by each assay.

<sup>b</sup> Percent of genotyped specimens with the correct SNP compared to the gold standard

\* McNemar's test measured a statistically significant difference ( $p < 0.001$ ) in genotyping accuracy between the Taqman assay and MCA

Interestingly, there were two clinical samples that displayed different melt curve profiles compared to the wild-type and mutant standards at codons 51 and 108. These curves resembled a hybrid form of the mutant and wild-type curves with two clear peaks at the lower temperatures (Figure 2.3). Sequencing confirmed that these samples contained a mixture of wild-type and mutant sequences at codons 51 and 108, indicating polyclonal infections.

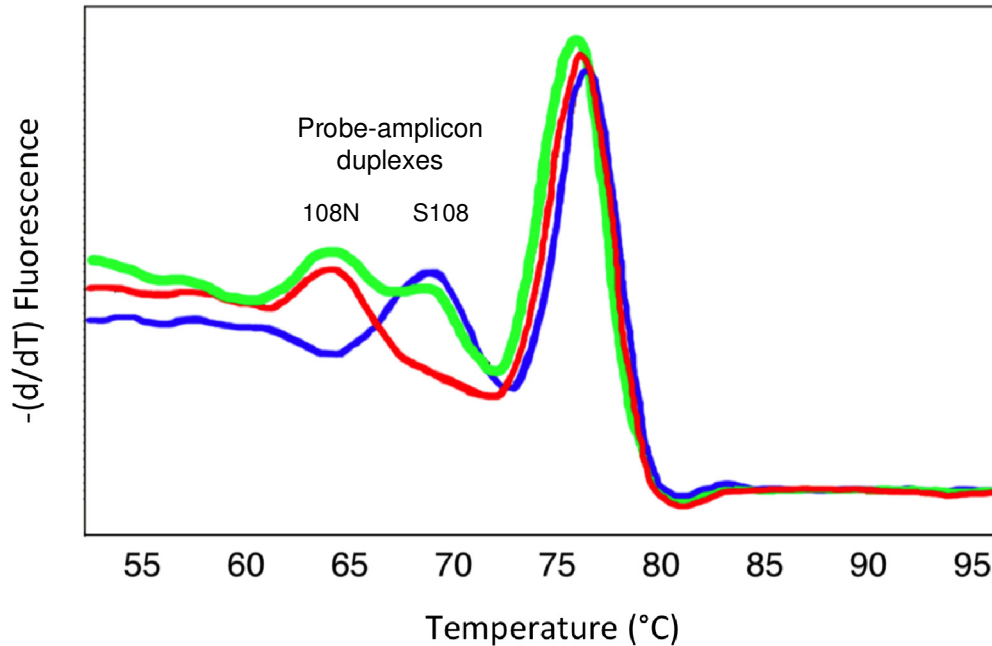


Figure 2.3 Genotyping of a mixed genotyped sample. Melting curve plot of one of the clinical samples with a mixed genotype (green) at codon 108 overlaid with melt curves from samples with the wild-type (blue) and mutant (red) SNPs.

*Pfdhps*: The same panel described above was used to evaluate the performance of the assay in its ability to genotype clinical samples by MCA. The sensitivity of the genotyping calling for each individual SNP was the following: 87.5% at codons 436/437, 96.8% at codon 540, 95.8% at codon 581, and 82.3% at codon 613 (Table 2.11). To determine the accuracy of the genotype assigned by MCA, each SNP was compared to the gold standard of direct sequencing. Concordance between MCA and direct sequencing ranged from 92% to 100% (Table 2.11). The 436/437 SNPs provided the lowest concordance due to its complicated ability to differentiate single wild-type/mutant combinations (much like sequence of 3D7 strain) particularly when the parasitemia is low. As mentioned, lowered

parasitemias lead to the generation of broad probe-amplicon peaks which reduces the ability of the software to distinguish wild-type/mutant combinations from the double mutants or wild-type sequences.

Table 2.11 Concordance between the MCA assay and the gold standard for genotyping the SNPs in the *pfdhps* gene

Codon	No. samples	No. detected	Sensitivity <sup>a</sup> (CI95%)	Concordance <sup>b</sup> (CI95%)
436/437	24	21	87.5% (69-96%)	90.5% (71-97%)
540	32	31	96.8% (84-99%)	93.6% (79-98%)
581	24	23	95.8% (80-99%)	91.7% (74-98%)
613	34	28	82.3% (66-92%)	100% (88-100%)

<sup>a</sup> Percent of total specimens that were genotyped by each assay.

<sup>b</sup> Percent of genotyped specimens with the correct SNP compared to the gold standard

### 2.3.4 Comparison of MCA and Taqman PCR for genotyping *pfdhfr*

In previous publications, Alker *et al.* reported a method using hydrolysis probes (Taqman technology) to discriminate between wild-type and mutant genotypes in the *pfdhfr* gene (3, 4). The sensitivity and specificity of genotyping the SNPs in the *pfdhps* gene by MCA was compared with the Taqman methodology as described. Primers and probes were initially validated using the constructed plasmids that contained either the wild-type (3D7) or mutant (V1/S) sequences at 10<sup>6</sup> copies of the *dhfr* gene. Poor specificity of the probes for the correct template was observed in this study as well as by others (57). In particular,

the wild-type probe for codon 59 bound indiscriminately to templates with the wild-type and mutant DNA sequences.

The panel of clinical samples was assessed using the Alker method. The sensitivity of genotype calling for the individual SNPs was as follows: 84.1% at codon 51, 93.2% at codon 59, 9.1% at codon 108, and 40.9% at codon 164. Of those specimens that could be genotyped, the concordance of Taqman real-time PCR with the sequencing methods was: 97.3% at codon 51, 25.6% at codon 59, 25% at codon 108, and 94.7% at codon 164 (Table 2.10). It is important to note that given the poor specificity of the probes for codon 59, all of the specimens were genotyped as wild-type whereas only 26% were confirmed as wild-type by sequencing.

## **2.4 DISCUSSION**

In this study a method was successfully developed for high-resolution MCA to genotype the major SNPs in the *pfdhfr* and *pfdhps* genes that are associated with resistance to pyrimethamine and sulfadoxine, respectively. Analytical validation of this assay demonstrated excellent sensitivity and specificity for both wild-type and mutant genotypes. The assay was further validated with a panel of clinical samples and demonstrated good concordance with sequencing methods. It is important to recognize that the panel of clinical samples consisted primarily of samples from returning travelers with low parasitemic infections. By microscopy, many of these samples had a parasitemia less than 0.1% (data not shown), suggesting that the level of parasite DNA was likely below the limit of detection of this assay.

However, in comparison with the published Taqman-based real-time PCR assay by Alker *et al.* (3, 4), the MCA assay demonstrated greater sensitivity and specificity for the genotyping of the SNPs in the *pfdhfr* gene. Although the reported sensitivity of the Taqman assay is 10 copies of the target DNA (3), this was not observed in this study nor from another laboratory that attempted to reproduce this method (2, 3, 57). Of significant concern, the poor specificity of the probes for codon 59 resulted in all of the panel samples being genotyped as wild-type when in fact 74% were confirmed mutant by pyrosequencing. The cross-reactivity between the wild-type and mutant probes in the Taqman assay precluded us from obtaining meaningful results for this SNP. This is especially problematic as the 51, 59, and 108 SNPs are the most commonly reported in many areas in Africa (86). The primers described by Alker *et al.* (2004) to genotype the SNPs in the *pfdhps* gene were tested using the conditions described. For each primer set, the amplified product was not detected, which may be attributed to the sub-optimal annealing temperature. It was anticipated that the poor PCR amplification would result in the poor genotyping capability of the Taqman probes. Furthermore, the Alker method requires that the investigator categorize the sample based on the cycle threshold ( $C_t$ ) values. This procedure can introduce bias and misinterpretation of results when competition occurs between probes. In contrast, MCA uses a relatively simple approach to genotyping, achieving high resolution and throughput capacity. The design of the assay facilitates its application to monitor mutations associated with other resistance genes. Resistance to cycloguanil, a metabolite of the antimalarial proguanil, is associated

with many of the same mutations in the *Pfdhfr* gene (62) enabling surveillance of resistance to this drug with the primers and probes described here.

Genotyping *pf dhfr* and *pf dhps* SNPs by MCA has been described elsewhere using fluorescence resonance energy transfer (FRET) methods (20, 49) but this assay requires an open system, as well as the use of labeled probes, in contrast to this method which uses less costly, unlabeled probes in a closed system. Another advantage of this assay is the ability to detect mixed infections. In highly endemic countries, people are likely to be infected with more than one strain of *P. falciparum* (78). Minor strains of polyclonal infections can be readily identified with this assay as two distinct probe-amplicon peaks. In this study, two infections that contained both a wild-type and mutant SNP at codons 51 and 108 were identified as mixed infections.

A similar assay for genotyping resistant *P. falciparum* has been developed using HRM with an intercalating dye analogous to LCGreen Plus. The HRM method uses the dissociation profile for each SNP to distinguish between wild-type and mutant sequences. However, the HRM analysis described by Andriantsoanirina *et al.* (5) does not use probes and has limited ability to resolve individual mutations that are located within close proximity on the DNA, such as the SNPs in *pf dhfr* codons 51 and 59 and *pf dhps* codons 436 and 437. HRM is best suited to genotype a single SNP per amplicon (37). Sequencing is another method that is widely used for genotyping and served as the gold standard for this study. However, limitations for high-throughput genotyping include the time required for processing samples (2 days compared with 4 hours with the MCA

procedure) and the need for PCR amplification prior to sequencing which risks contamination by amplicons.

MCA will be a useful tool for molecular surveillance of resistant genotypes within endemic populations with higher parasitemic infections. It can be implemented to monitor the efficacy of antimalarial drugs, and in particular, the emergence of drug resistant strains in pregnant women undergoing Intermittent Preventative Therapy. This high-throughput assay enables rapid screening of large numbers of samples and provides a new tool to support efforts for malaria surveillance and elimination. Once applied to a broader selection of resistance genes, the technique presented here can be useful to identify global changes in resistance patterns for malaria.



## Chapter 3 Application of the MCA assay to in-gel PCR technology

### 3.1 Introduction

In many endemic areas, health care workers readily prescribe an antimalarial based on febrile symptoms, partially due to the fact that malaria rapid diagnostic tests are not available in some rural areas (12). One of the key strategies for improved case management is to refer suspected cases for laboratory testing prior to providing prescriptions. Many health facilities do not have the laboratory capacity to perform the confirmation because of lack of resources (75). Patient care among parasite-positive patients can be improved by utilization of a testing device, specifically a point-of-care (POC) testing tool to diagnose *Plasmodium* infections. POC tests that also genotype parasites would further support the surveillance of drug-resistant strains among populations living in high transmission areas. Results from surveillance studies can provide evidence for policy makers when deciding on effective drug regimens. In the absence of sensitive surveillance tools, resistance against antimalarials remains unrecognized and perpetuates the transmission of disease.

New developments in POC technologies are focused on the miniaturization of PCR platforms to bring molecular diagnostics and genotyping to the field setting. These platforms are both easy to use and inexpensive. In 2010, Atrazhev *et al.* described a method, known as in-gel PCR, that allows PCR to take place within a colloidal gel matrix (6). In this method, real-time PCR and melting curve analysis (MCA) are both conducted on “molecular polonies”, or an array of gel posts, which are anchored to a glass coverslip. Each post is approximately 1  $\mu$ L

in volume, which minimizes the amount of reagents and the costs required. This chapter reports on the application of the *Plasmodium falciparum* genotyping assay developed on the LightCycler® onto the platform described by Atrazhev *et al.* (2010).

## **3.2 Materials and methods**

### **3.2.1 DNA template**

Plasmids containing the 641 bp region of the DHFR gene from *P. falciparum* 3D7 and V1/S genomic DNA were previously described in Chapter 2 (Section 2.2.1). These *pfdhfr* plasmids ( $10^6$  copies) were used to optimize in-gel PCR. The DNA template was added to the PCR mixture prior to gel polymerization; however, Atrazhev *et al.* (2010) indicate that the DNA can be added post-polymerization. For the validation of this assay on the gel post system, the template was included in the gel-PCR mixture.

### **3.2.2 In-gel PCR of *pfdhfr* codon 108**

In-gel PCR of codon 108 of the *pfdhfr* gene was performed using 47  $\mu$ L of the PCR reagents plus the following gel reagents: 4% acrylamide (Sigma, cat no. A9099) + 4% bis-acrylamide aqueous solution (*N,N*-methylene bisacrylamide, BioRad, Hercules, CA, cat no. BA05-1610201), 0.12% azobis (2,2'-azobis(2-methyl-*N*-(2-hydroxyethyl) proprionamide), Wako, Richmond, cat no. VA-086), and 0.1% TEMED (*N,N,N',N'*-tetramethylethylenediamine, Sigma, cat no. T7024). The 47  $\mu$ L of the PCR reagents were previously described in Chapter 2 (Section 2.2.3).

PCR performed on the gel posts required a highly concentrated (12 U) *Taq* polymerase along with buffers 10X UB4 (500 mM tris-sulfate, pH 8.6, 160 mM (NH<sub>4</sub>)<sub>2</sub>SO<sub>4</sub> (Sigma); 50 mM H<sub>3</sub>PO<sub>4</sub> (Sigma); and 1% Tween20 (Sigma)) generously provided by Dr. Atrazhev. Prior to adding the other PCR and gel reagents, 1X UB4 buffer was mixed with 3.5 mM MgSO<sub>4</sub> to form a precipitate. This precipitate enables for the reaction to have a synchronized start and activation of the *Taq* enzyme when the Mg<sup>2+</sup> ions dissolve.

### **3.2.3 Polymerization of PCR reagents**

*Within test capillaries:* PCR reagents were mixed with polymerization reagents in LightCycler® capillaries using a photochemical method, whereby the capillaries were exposed to UV light for 20 minutes. In this method, long wave ultraviolet light catalyzes the polymerization with ‘azobis’ to form the gel matrix.

Unpolymerized reagents potentially inhibit the PCR; thus after the polymerization process, the aqueous upper layer in the capillary was removed and discarded.

*On free-standing gel posts:* PCR reagents in addition to the gel reagents were spread over the opening of the glass mold and covered by a treated glass coverslip. The mold itself is constructed from two glass microscope slides that are permanently bonded together (Figure 3.1, panel A). One of the slides has an 8 x 6 array of holes; each hole creates the cylindrical structure of the gel posts. The array was exposed to the long-wavelength UV light for approximately 20 minutes, after which the coverslip was carefully separated from the mold so as to detach the posts. The self-standing gel posts were submersed in immersion oil (face-up) in a shallow 23 x 23 mm anodized metal pan.

*Gel posts in molds:* Unlike the free-standing gel posts, PCR reagents polymerized within the gel molds were not detached. The coverslip was carefully removed after the polymerization and the mold was placed into the anodized pan, with the top surfaces of the posts facing down to reduce dehydration.

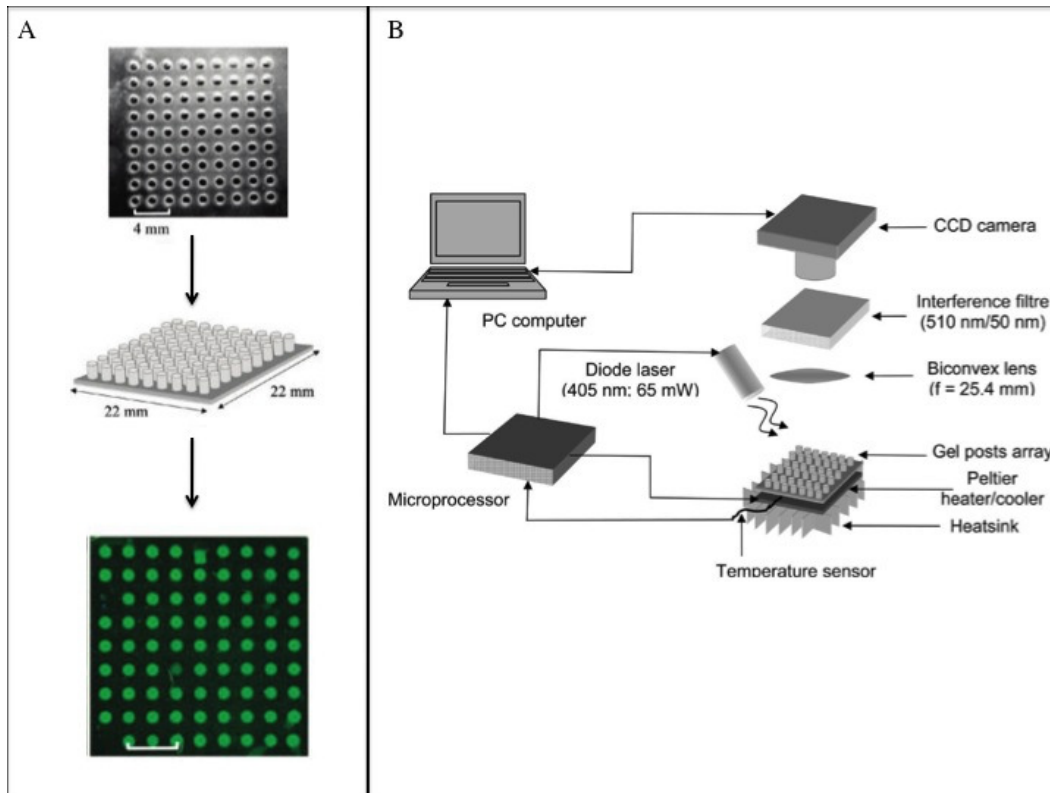


Figure 3.1 Operational diagram of the in-gel PCR prototype system. Schematic of (A) gel post arrays and (B) the Viriloc system, which is the prototype instrument used to perform in-gel PCR and MCA. *Figures adapted from Atrazhev et al. (2010).*

### 3.2.4 PCR process

*LightCycler®:* In-gel PCR was performed on the LightCycler® using the following parameters: hold at 95 °C for 2 minutes; 40 cycles of 95 °C for 30 s, 48 °C for 30 s, and 72 °C for 30 s. Post-extension immediately after the 40 cycles was set at 72 °C for 10 minutes. Ramp rates for denaturation, annealing, and

extension were set at 20 °C/s, 3 °C/s, and 0.1 °C/s, respectively. After post-extension, MCA was performed as follows: 95 °C for 30 s; 55 °C for 1 min, with a ramp rate of 0.01 °C/s; and final denaturation at 95 °C for 30 s. The software program on the LightCycler® (version 4.1) was used to identify samples based on the melt-curve profiles. External standards, described in Chapter 2, were used to genotype the samples.

*Viriloc*: The prototype instrument, previously described by Atrazhev *et al.* (2010), was used to perform PCR and MCA on the gel posts using the same parameters as described above. This instrument will be referred to as “Viriloc” throughout the rest of this thesis (Figure 3.1, panel B). Thermal settings can be programmed into the Viriloc to replicate the temperature settings from the LightCycler®. However, the ramp rates are not adjustable on the Viriloc system and were confined to approximately 1.4 °C/s for all the steps of the PCR. The MCA process was similar to the program described by the LightCycler® method above.

A CCD camera captured images of the fluorescing posts at each extension cycle of the PCR and at each temperature step of the MCA. These pictures were saved to the attached computer and later analyzed for PCR critical threshold and MCA melting peaks. Fluorescence emitted from each post was analyzed by ImageJ software (National Institutes of Health, U.S.).

### **3.3 Results**

#### **3.3.1 LightCycler® in-gel PCR**

To determine the compatibility of the genotyping assay with the in-gel technology, the gel reagents were added to the PCR reagents and UV polymerized within LightCycler® capillaries. The in-gel PCR was tested within the capillaries with the LightCycler® cycling conditions. Figure 3.2 illustrates the melting peaks for the in-gel PCR performed at the original ramp rate settings. Both symmetric and asymmetric PCR (performed without the probe) were tested to ensure that the primers were capable of amplifying *dhfr* codon 108 within the gel matrix. Regardless of the gel concentration, in-gel PCR generated a lower yield of amplicons compared to liquid PCR.

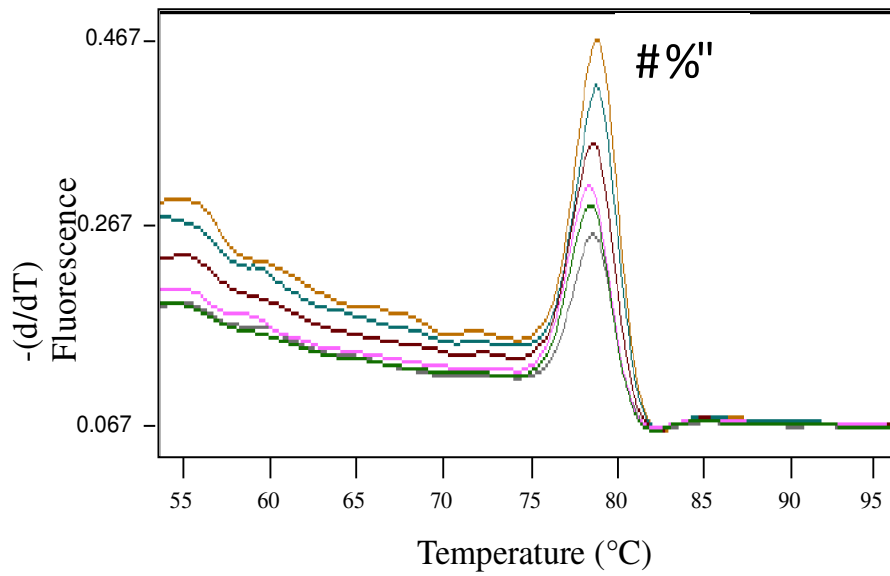
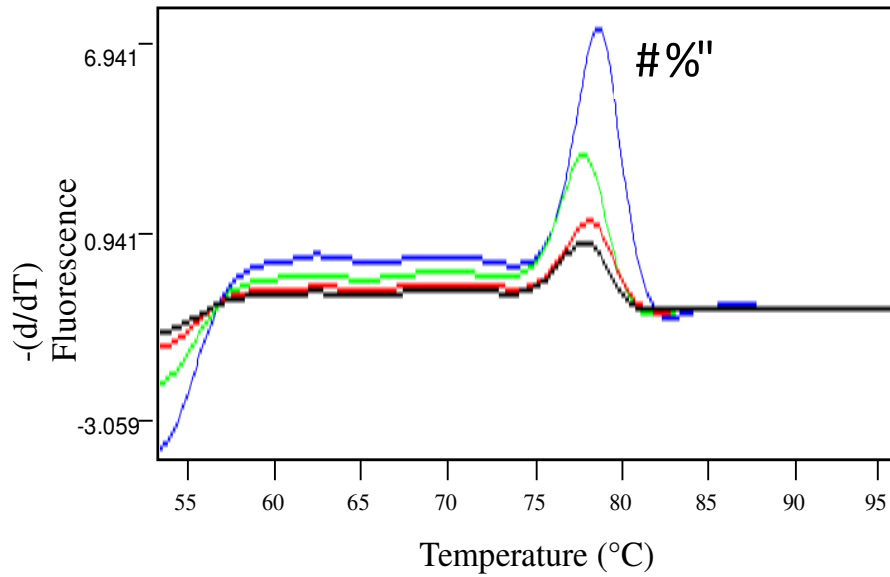


Figure 3.2 Melting curve plots of replicate reactions of in-gel PCR performed on the LightCycler® for *pdfhfr* at codon 108 using 3D7 plasmid DNA. The original LightCycler® conditions were tested for (A) symmetric PCR and (B) asymmetric PCR with the excess reverse primer. AD = amplicon duplex.

### 3.3.2 Genotyping from in-gel PCR on the LightCycler®

Addition of the probe to the asymmetric PCR was tested to determine the capacity for genotyping within the gel matrix. Although the fluorescence intensity decreased, distinguishable probe peaks were detected and corresponded to the correct genotype (Figure 3.3).

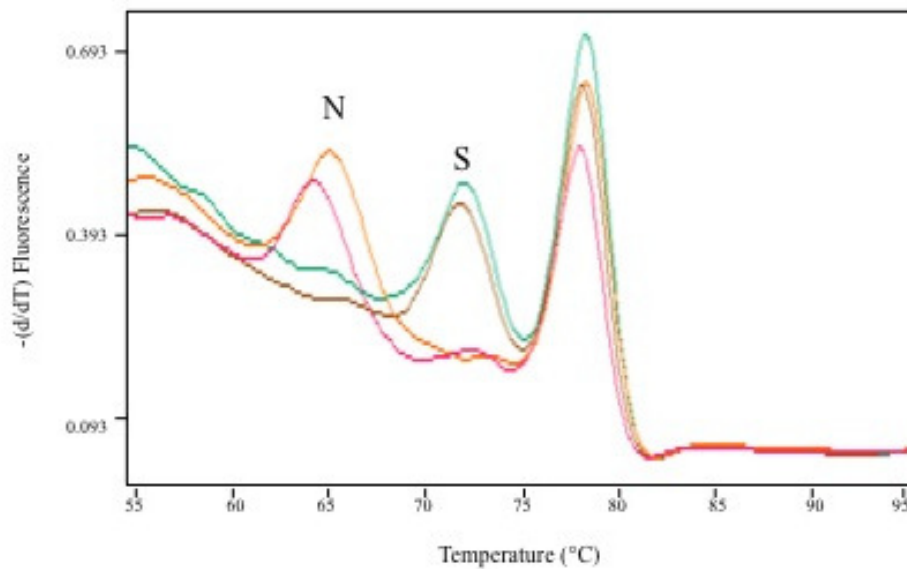


Figure 3.3 Melting curve plots from genotyping at SNP S108N of the *pfdhfr* gene by in-gel PCR performed within the LightCycler® capillaries. 3D7 and V1/S plasmid DNA was tested for the wild-type and mutant alleles, respectively, for the 108 codon. The genotyping peak for the wild-type allele (S) has a higher melting temperature than the peak for the mutant allele (N).



### 3.3.3 In-gel PCR on the Viriloc

Early attempts to perform symmetric in-gel PCR were successful (Figure 3.3 A) generating a product of the correct amplicon size (Figure 3.3, panel B). However, in all subsequent experiments, this PCR reaction either failed completely or produced primarily primer-dimers (Figure 3.3, panels C and D). Similarly, asymmetric PCR without or with the probe produced primer-dimers precisely where we expect to see the genotyping peak (Figure 3.4).

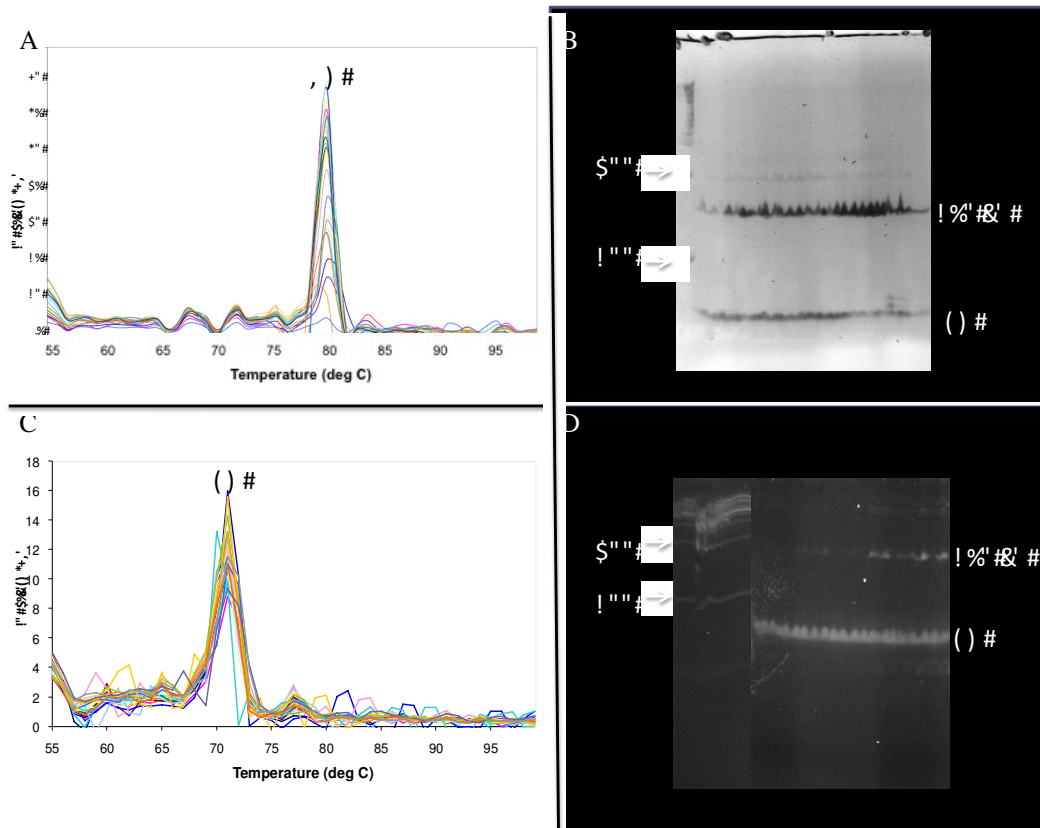


Figure 3.4 Melting curve profiles and gel electrophoresis of in-gel PCR products following amplification and melt curve analysis on the Viriloc. Size confirmation of amplified products from each individual gel post run on a vertical polyacrylamide gel (100bp ladder shown on the left). Amplicon duplex (AD) is 150 bp in size; the primer-dimer (PD) is less than 100 bp.

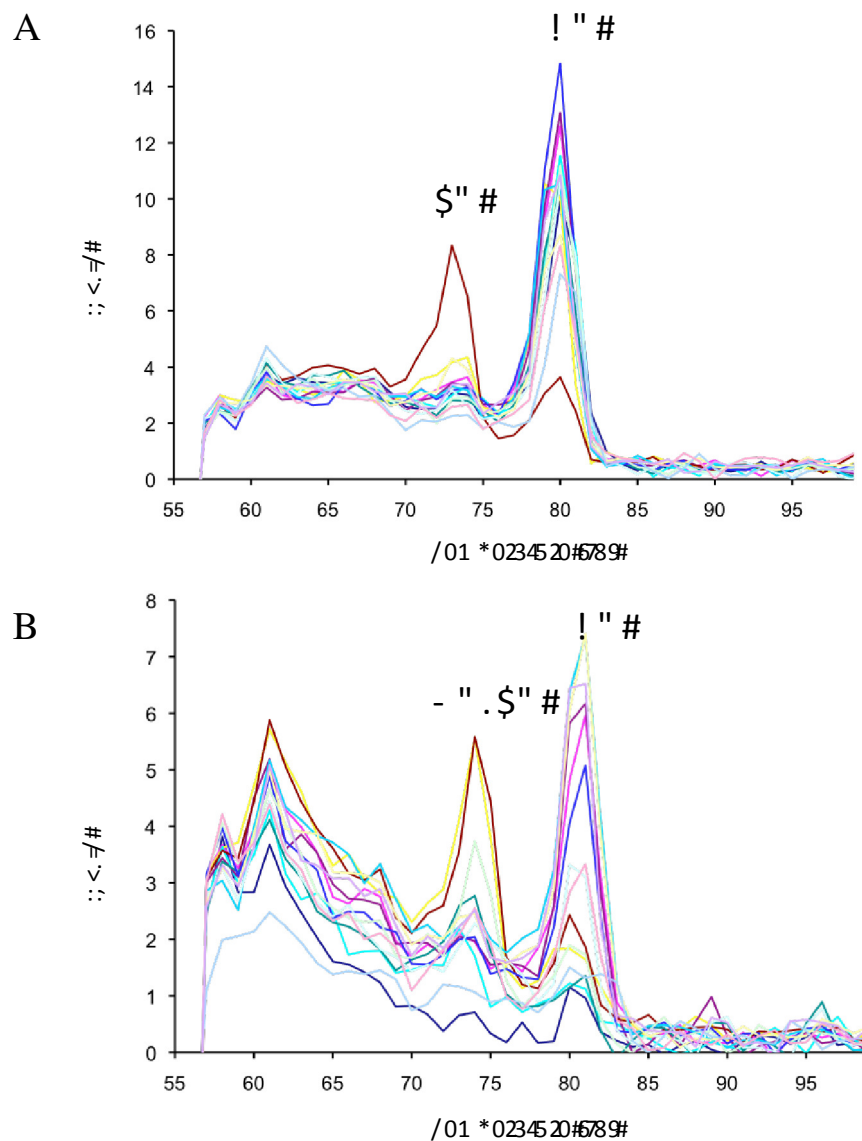


Figure 3.5 Melting curve plots of asymmetric in-gel PCR without (A) and with (B) probe performed on the Viriloc. Products that melt at 80 °C correspond to full-length amplicons (AD= amplicon duplex peak), whereas primer-dimers melt at 73 °C.

### 3.3.4 Ramping rates

The ability to genotype with this method depends on the detection of the probe-amplicon duplex at lower melting temperatures. When the PCR reaction is inefficient, primer-dimers or non-specific amplification products will also melt in

this low temperature range. One factor that affects the efficiency of the PCR is the ramping rate of the PCR system. Ramp rate is defined as the change in temperature per second. Primers will anneal to the template as the PCR is ramping down, or cooling, from the denaturation to the annealing temperature. Primers can be extended as the PCR is ramping up from the annealing temperature. On the LightCycler®, the ramping rate was set to 20 °C/s, 3 °C/s, and 0.1 °C/s for denaturation, annealing, and extension, respectively; whereas on the Viriloc, the ramp rate was approximately 1.4 °C/sec for all three steps.

To test whether ramp rate contributed to primer-dimer formation on the Viriloc system, PCR was performed in the LightCycler capillaries set to the Viriloc ramp rates. A symmetric in-gel PCR was used as a control to determine if the primers would normally anneal to each other when there were equal concentrations of both primers. For both symmetric and asymmetric PCR, the melting curve profile produced two peaks (Figure 3.5). One peak corresponds to the amplicon, while the second peak is at 71-72 °C, which unfortunately overlaps with the expected probe-amplicon peak. Since this extra peak was not observed with the LightCycler ramp rates, the second peak could be generated as a result of decreasing the ramp rate.

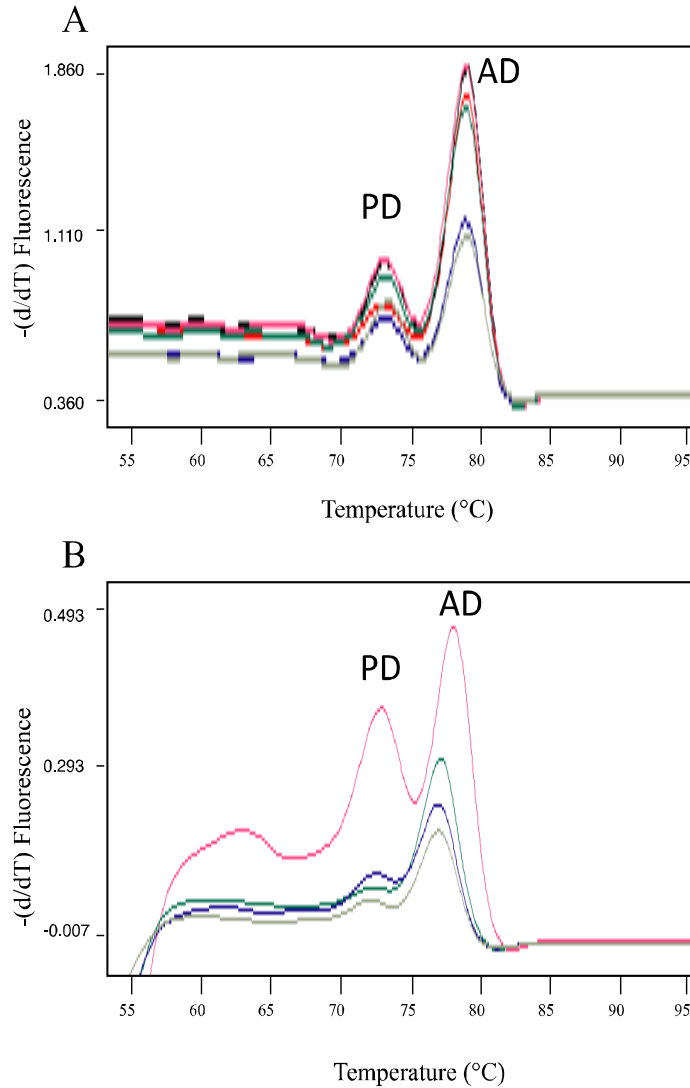


Figure 3.6 Melting curve profiles from in-gel PCR of a plasmid with the wild-type sequence at codon 108 in the *pfdhfr* gene performed in capillaries on the LightCycler® tested with the Viriloc ramp rate settings for (A) symmetric and (B) asymmetric PCR without probes. AD = amplicon duplex peak; PD = primer-dimer peak.

To find out if genotyping is compatible with the in-gel technology, the *pfdhfr* probe for codon 108 was polymerized with the gel reagents and the asymmetric PCR and MCA was performed on the LightCycler® using the Viriloc ramping rates. A distinguishable probe peak was produced at the corresponding

melting temperatures for the wild-type and mutant sequences (Figure 3.6, panel A). To determine whether the ramp rates are a major contributor to the formation of primer-dimers, the asymmetric in-gel PCR polymerized with the probe was tested on a Viriloc system for both the wild-type and mutant sequences. The melting curve profile generated by the Viriloc system indicated a 1-degree difference between the wild-type and mutant amplicon-probe peaks (Figure 3.7, panel B). This result indicates that when the probe is added to the asymmetric in-gel PCR reaction, primer-dimers are not predominant as observed in previous experiments but they cannot be ruled out completely. This result further suggests that there may be other factors aside from the ramp rate that contribute to the formation of primer-dimers.

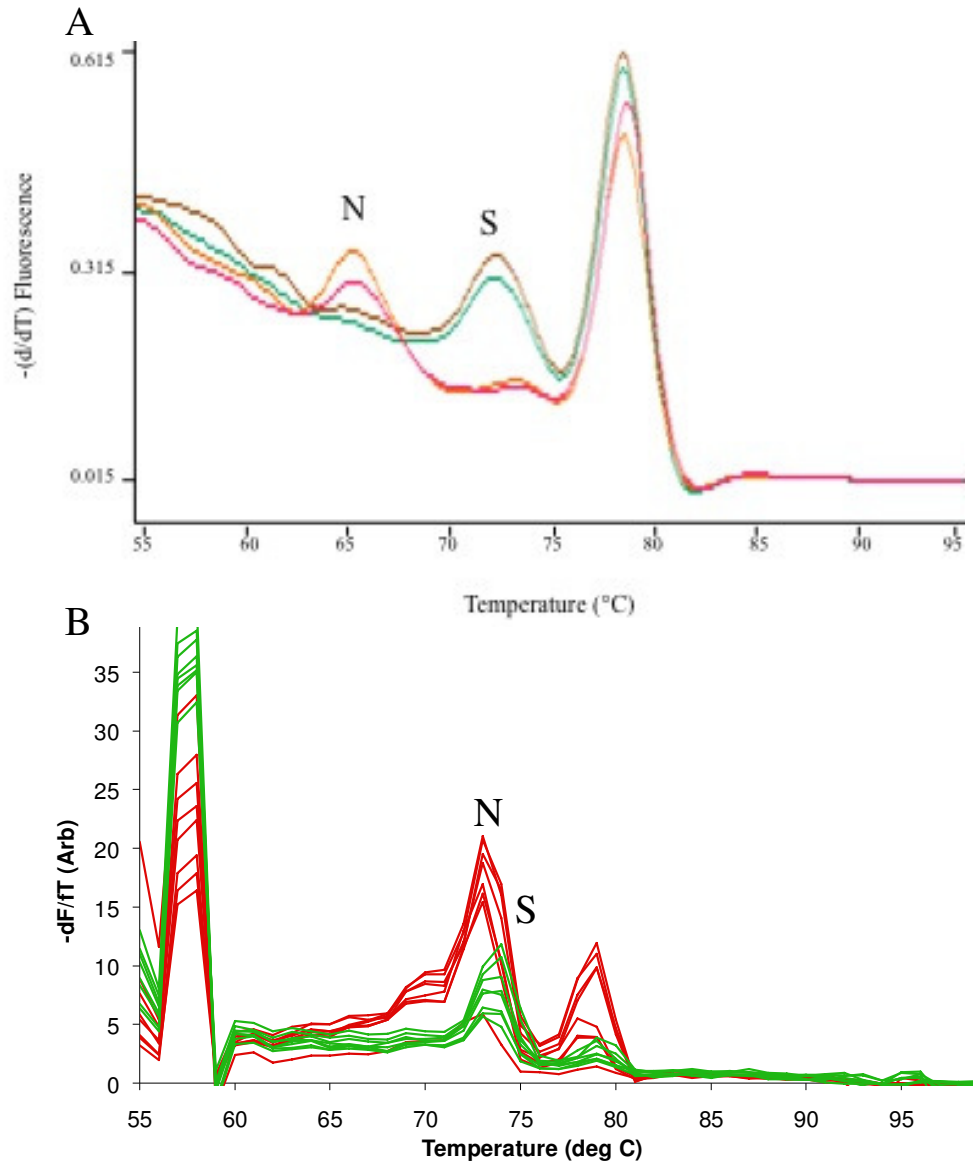


Figure 3.7 Melting curve plots to genotype *P. falciparum* plasmid DNA with the wild-type (S108) and mutant (108N) sequences using the Viriloc ramp rate settings on (A) the Lightcycler® and (B) the Viriloc system. S = wild-type at codon 108; N = mutant at codon 108.

### 3.3.5 Gel concentration

The pore size of the acrylamide gel can also be a factor that influences the amplification of non-specific primer-dimers. A smaller pore size can theoretically inhibit the movement of primers, thus preventing the reaction from producing amplicon products, whereas a larger pore size can allow for hairpin structures to form, which can also prevent primers from annealing to the appropriate complementary sequence. To determine the effect of pore size on amplification, several experiments were performed on the LightCycler® in which the capillaries contained a gel percentage ranging from 4% to 6% in addition to the PCR reagents. Reaction capillaries with higher percent polyacrylamide content will have comparably smaller pore sizes. With the LightCycler® ramp rates, the Ct values were found to be consistent across the range of percent acrylamide, which is indicative of no effect on the PCR itself. The same assay was tested with the LightCycler® programmed for the Viriloc ramp rate. The Ct values from the PCR also remained consistent; however, the MCA indicates that there was non-specific binding as a primer-dimer peak (Table 3.1). These results suggest that the primer-dimers are more likely to be generated under the combined conditions of a low ramp rate and a gel matrix.

Table 3.1 Summary of factors that contribute to the generation of primer-dimers.

Factor	LightCycler ramp rate*		Viriloc ramp rate*	
	Symmetric PCR	Asymmetric PCR	Symmetric PCR	Asymmetric PCR
Gel concentration	NPD	NPD	PD	PD
Residual unpolymerized gel	NPD	NPD	NPD	PD
Annealing temperature	NPD	NPD	PD	PD
Excess forward primer	n/a	NPD	n/a	NPD

\*All reactions performed in duplicate  
 PD, primer-dimer; NPD, no primer-dimer; n/a, not applicable

### 3.3.6 Unpolymerized polyacrylamide inhibition

It is possible that up to 10% of the polyacrylamide gel posts remains unpolymerized (68). Unpolymerized acrylamide is a PCR inhibitor, which could prevent the amplification of a DNA product. To determine the level of PCR inhibition from unpolymerized gel reagents, the upper aqueous liquid layer was not removed after polymerization. This was compared against 1) a capillary where the layer was removed and 2) a capillary where the layer was removed and 2  $\mu$ L of the original mastermix (left unpolymerized) was added back. Primer-dimers were produced under the Viriloc ramp rates, most notably when the layer was not removed (Table 3.1). This result suggests that at lowered ramp rates, asymmetric in-gel PCR is affected by the unpolymerized gel reagents, which then



culminates in the production of primer-dimers. Similarly, asymmetric PCR is more sensitive to PCR inhibition from the unpolymerized acrylamide.

### **3.3.7 Annealing temperatures**

Non-specific amplification can occur if the annealing temperatures are set at sub-optimal values. Asymmetric PCRs (without the probe) performed on the Viriloc systems were tested at various annealing temperatures to reduce the primer-dimers. The non-specific product peak was present across the range of temperatures tested (Table 3.1) when tested on the LightCycler® with the Viriloc ramp rate settings. This primer-dimer will affect the ability to genotype the sample when the probe is added to the reagent mixture. To determine the optimal annealing temperature, a gradient PCR with the asymmetric mastermix was performed. The annealing temperature was tested from 48 °C and 58.7 °C. A single band, indicative of the amplicon peak, was present at all temperatures in this range (Figure 3.8). This shows that the annealing temperature does not contribute towards the development of the primer-dimers.

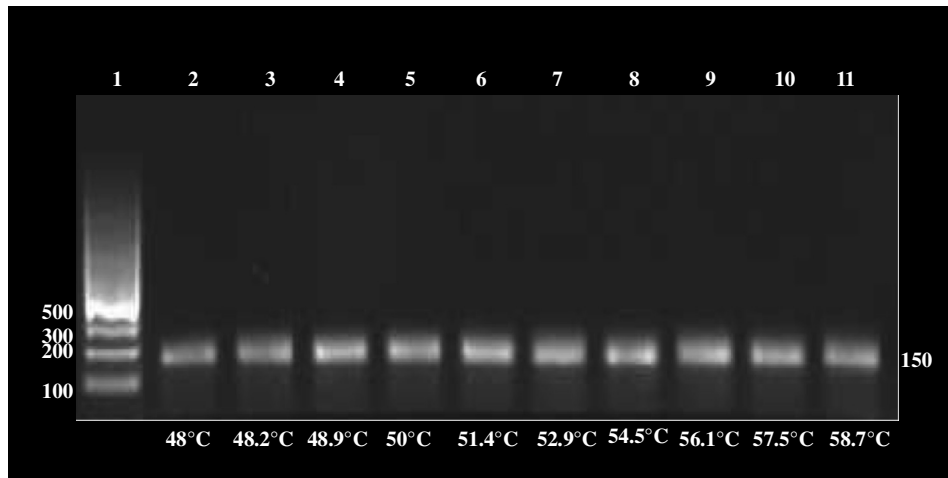


Figure 3.8 Gel electrophoresis of the asymmetric PCR reaction of plasmid DNA with the wild-type sequence for amplification of *pfadhfr* SNP S108 using an excess of the reverse primer performed on the gradient thermocycler. Lane 1 contains the DNA ladder; lanes 2 to 11 show a single amplicon product of 150 bp generated when the annealing temperature ranged from 48 °C to 58.7 °C.

### 3.3.8 Hairpin structures

A primer can fold back on itself and allow the complementary nucleotides to form duplex structures. These hairpin structures can lead to the formation of non-specific amplicons. These hairpin structures were not shown on the gradient PCR, nor were they problematic with the original LightCycler® assay. It is possible that the colloidal matrix of the gel is conducive to the formation of hairpins. To test this phenomenon, the primer ratio was changed such that there was an excess of forward primer and conversely, the reverse primer was limiting. This asymmetric in-gel PCR was performed on the LightCycler® and tested with two types of ramp rates. Regardless of the gel concentration and ramp rate, no primer-dimers were generated (Figure 3.9), suggesting that the excess forward primer is less prone to forming structures that result in primer-dimers.

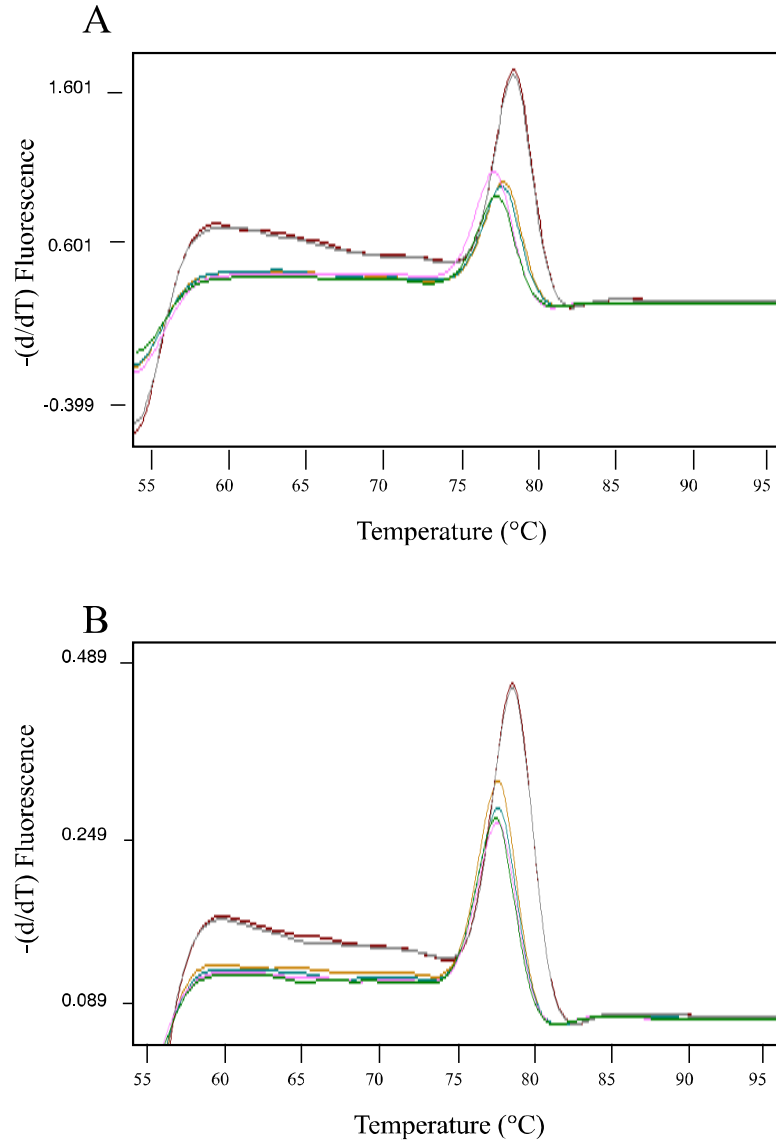


Figure 3.9 Melting curve profiles for asymmetric in-gel PCR of plasmid DNA with the wild-type sequence for *pfadhfr* SNP 108 with an excess of the forward primer tested on the LightCycler®. No primer-dimers were generated with either the LightCycler® ramp rate (A) or the Viriloc ramp rate (B).

### 3.4 Discussion

In-gel PCR is achievable on the LightCycler® for symmetric reactions but inconsistencies with asymmetric in-gel PCR were observed. Asymmetric in-gel PCR with the excess reverse primer generates primer-dimers, which may be

attributed to its sensitivity to ramping rates, the confined structure of the gel matrix, excess primers forming hairpin structures, and PCR inhibition caused by residual unpolymerized polyacrylamide. The combination of these factors can enhance the susceptibility to generate primer-dimers and thus reduce the efficiency of amplification. These primer-dimers were not detected when the ramp rate was set to the original LightCycler® settings. Similarly, an asymmetric PCR with an excess of the forward primer did not produce detectable primer-dimer peaks, regardless of the ramp rate setting.

The results from the in-gel PCR performed within the LightCycler® capillaries showed the potential to amplify and genotype products within the gel matrix. The assay developed thus far needed to be applicable to PCR performed with the Viriloc instrument. In-gel PCR can take place either within the glass mold or as free-standing gel posts on a glass coverslip. With the exception of two experiments, the PCR efficiency was poor when tested on the Viriloc. The experiments that did show successful amplification on the Viriloc system require further confirmation.

Primer-dimers can be caused by numerous factors: type of *Taq* used, magnesium concentration, annealing temperature, and ramp rates. The more concentrated *Taq* polymerase enzyme, known as “*Taq* 2000,” produced stronger melting curve peaks, which is indicative of an efficient PCR. *Taq* 2000, developed by Dr. Atrazhev in 2000, is a DNA polymerase that is four times more concentrated than the commercial Platinum *Taq*. There are two buffers that will enhance the efficiency of *Taq* 2000: UB1 and UB4. The latter buffer, also

developed by Dr. Atrazhev, requires the addition of  $MgSO_4$  to be mixed prior to the addition of the other PCR and gel reagents. A precipitate forms when UB4 and  $MgSO_4$  are added together. This magnesium in the precipitate is absolutely necessary for the *Taq* to be effective in DNA synthesis. However, the distribution of the PCR and gel reagents across the mold becomes difficult to spread the precipitate equally among the wells. Unequal distribution of magnesium will have an influence on the activity of the *Taq* and may contribute to the production of primer-dimers. However, regardless of the reagents, the final product is ultimately dependent upon the system that carries out the reaction.

One of the major differences observed between the LightCycler® system and the Viriloc system is the non-modifiable ramping rate. This rate varies between the different Viriloc systems. It is suspected that the ramp rate is inconsistent from the beginning to the end of the cycling steps of the PCR. As well, it is hypothesized that the ambient room temperature affects the system ramp rate, such that at lower room temperatures, the system ramp rate will decrease. Room temperature could not be controlled; for example, other systems that were running simultaneously added to the hot environment. The inconsistent ambient room temperature may be a contributor to the variations observed in the outcomes of the PCR when run on a Viriloc system.

The temperature heating and cooling rates are thought to affect the specificity of amplification. At lowered ramping conditions, the primers are allowed to anneal to non-specific sites, including sequences within it. This is because there is ample time for primers to bind to areas outside of the desired

amplicon region. As a result, the PCR produces extraneous amplified products, which are identified as primer-dimers. The primer-dimers have different lengths compared to the amplicon, and this produces a lowered melting curve.

Unfortunately, the melt curve of the primer-dimers is approximately the same temperature as the genotyping (probe-amplicon) peak.

Development of a genotyping assay that can be used in the field would be a significant advance to control the rampant spread of drug-resistant *P. falciparum*. The genotyping assay developed on the LightCycler® can contribute to the surveillance of SP resistance, and easily be applied towards other genes that confer resistance to antimalarials. The limitation in using the LightCycler® system is the requirement for large, expensive machinery and the training and expertise of personnel. These heavy demands encourage the generation of POC technologies, such as the Lab-on-a-Chip.

In-gel PCR is a promising technology that allows for small-scale PCR reactions to take place within a gel matrix using an inexpensive and potentially portable device. This method moves closer towards bringing molecular testing to the field. In order to use this method in malaria endemic areas, the feasibility of the genotyping assay needed to be tested. The in-gel PCR performed in the LightCycler® capillaries indicate that genotyping within the matrix is possible but not with the current Viriloc system.

It appears that in-gel PCR is susceptible to forming stable hairpin structures, which may be attributed to restricted confinement of the gel pores.

Primer-dimers are by-products of the spatial environment that encourages the oligonucleotide to fold and maintain a particular secondary structure. Primer design is an important element for all future assays using in-gel PCR.

The results from the in-gel PCR performed in the capillaries highlighted the importance of the heating capacity of the system. The PCR itself is highly dependent upon the thermal conditions. The Platinum *Taq* polymerase is dependent upon reaching high temperatures to allow for the deactivation of the antibody as well as the denaturation of the template. The engineers and researchers who have been working on the development of the Viriloc often measured variable heat signatures from the system. Some of these heat signatures are not achieving the temperatures programmed, which can affect the activity of the polymerase. Given the requirement for consistent ramping rates and heating, the current model of the technology is the limiting factor in the ability to genotype drug-resistant malaria.

## Chapter 4: Discussion and conclusions

This work demonstrates that single nucleotide polymorphisms (SNPs) in the *Pfdhfr* and *Pfdhps* genes can be detected using a closed, high-throughput method on the LightCycler® platform. Genotyping within a hydrogel matrix, as performed with the in-gel technology, is possible but the major prerequisite for the in-gel technology is a functional platform on which the PCR and MCA will be tested. While the platform is undergoing further developments, the high-throughput method on the LightCycler® has a number of immediate applications both in non-endemic and endemic areas.

### 4.1 Application of the LightCycler® assay for surveillance

Technological advances to support malaria surveillance programs will be invaluable for large-scale epidemiological studies that guide policy makers on antimalarial drug efficacy. Since SP is widely used as the chemoprophylaxis for intermittent preventative therapy (IPTp) during pregnancy, policy makers can utilize the outcomes from molecular surveillance studies to direct their decisions regarding the replacement of SP. Impaired immunity during pregnancy is a contributor to drug resistance by reducing the ability of the host to clear a malarial infection (50). The long-elimination half-life of SP suggests that newly acquired *P. falciparum* infections are exposed to low concentrations of the active drug. This terminal elimination phase is deemed responsible for the selection of resistant parasites (79). In a study that observed the prevalence of resistant alleles post-IPTp, pregnant women who had undergone IPTp showed increased carriage of *P. falciparum* with resistance alleles in the *dhfr* and *dhps* genes (31). These



results support the “competitive facilitation” model, whereby SP-resistant parasites over-grow the susceptible strains when subjected to chemotherapeutics. Given the selective pressure of antimalarials on parasites, it is important to monitor the efficacy of SP through surveillance of the molecular markers associated with resistance.

The development of the genotyping assay on the LightCycler® will be useful for surveillance of drug resistance for countries that follow the WHO recommendation of using SP for IPTp. Uganda is one of many developing countries that use SP for IPTp. A current study by our group, in collaboration with Dr. Anthony Mbonye from the Ministry of Health in Uganda, is investigating the effectiveness of SP among pregnant women on IPTp in Uganda. One of the main objectives of the study is to determine the prevalence of parasites with haplotypes associated with resistance to SP. The outcomes of this study can potentially provide evidence required to make policy changes regarding prophylaxis treatment during pregnancy.

Specifically, women enrolled in the study will provide blood samples at three intervals during pregnancy. These blood samples will be acquired prior to receiving the two doses of SP during the second and third trimester; and the final sample will be taken at the time of delivery. Samples that are positive by microscopy will be further genotyped using the high-throughput method described by Cruz *et al.* (2010) to assess resistance (16). Typing for the resistant alleles among the pregnant women will be performed at the Uganda Virus Research Institute (UVRI), located in Entebbe, Uganda. This government public health

research institution is involved with various clinical trials and intervention studies. The UVRI is committed to researching infectious diseases and advising the Ministry of Health regarding issues surrounding health policy and control strategies for disease control and prevention (71).

#### **4.1.1 Building laboratory capacity in Uganda**

For the most part, clinical research tests have been widely used in developed countries, but there is poor transference of these methods to developing countries that need them most. In July of 2010, the research team from the University of Alberta provided a workshop at the UVRI for training on the genotyping method presented in this thesis. There were two primary objectives for the workshop: 1) to train laboratory staff in molecular biology and specifically, how to perform the genotyping assay, and 2) to identify cost savings in the methodology to ensure that this assay can be integrated into national surveillance programs over the longer term. The assay on the LightCycler® will first be applied to our clinical study by genotyping the samples in the local laboratory where malaria is endemic. This transference of the assay to UVRI will also provide an important opportunity to enhance laboratory capacity in this endemic region.

Training in how to perform the assay constituted a major part of the capacity building program for the Ugandan research team. It strengthened the team members' skills and competencies to use new technologies for surveillance. Some of the members of the research team at the UVRI were new to using a real-time PCR platform. Part of the training with the protocol required that the

researchers become comfortable with using the system, and understanding the methods for optimization. The transfer of the protocol from the LightCycler® 2.0 to the LightCycler® 480 platform also required some of the genotyping reactions to be optimized for efficiency.

At the UVRI, real-time PCR platforms have been minimally used and only for select studies. The workshop enabled many users to become acquainted with the programs and capabilities of the system. Such technically advanced systems are daunting and intimidating for first-time users. The technical workshop provided support to these users, as well as encouragement to develop other future assays.

The assay, as presented in Chapter 2, was originally designed on the LightCycler® 2.0 platform, which has a maximum capacity of 32 samples. The platform available at the UVRI was the LightCycler® 480, which performs real-time PCR and MCA from a 96-well plate. The high sensitivity of the system allowed the research team to decrease the total reaction volume from 20  $\mu$ L to 10  $\mu$ L. The reduction in reaction volume implies that less *Taq* polymerase will be added to the mixture. *Taq* polymerase is the most expensive reagent in the mixture; thus, the reduction in volume will inevitably reduce the cost associated with performing each test. Another effort to reduce costs was to change from using the expensive Platinum *Taq* to utilizing a more cost-efficient *Taq* polymerase.

#### 4.1.2 Surveillance programs in Uganda

Malaria control programs in Uganda have been highly dependent upon the data collected from health facilities, which is primarily clinical diagnosis without laboratory confirmation. In order to address poor linkages between treatment practices and laboratory test results, Uganda has established a network of researchers, policy-makers, and key-stakeholders, all of whom contribute to evidence-based national policy for antimalarials. The Uganda Malaria Surveillance Program (UMSP) was established in 2001 to monitor efficacy of antimalarial therapies, antimalarial-related adverse events, disease-associated morbidity and mortality, and the pharmacovigilance of antimalarials. The UMSP has implemented laboratory diagnosis and molecular surveillance at multiple sentinel sites. At these “centers for excellence”, the current method for genotyping *P. falciparum* for SP resistance is by nested-PCR. The LightCycler® genotyping assay that is implemented at the UVRI aligns well with the UMSP laboratory activities, specifically the monitoring of antimalarial resistance through molecular markers. This high-throughput method can therefore facilitate genotyping at the UMSP sentinel sites and provide more sophisticated testing at lower cost.

As part of the UMSP, the LightCycler® assay would be beneficial in monitoring the prevalence of SNPs associated with SP resistance. The collaboration of the UMSP with the Prevention of Malaria and HIV Disease in Tororo (PROMOTE) study group will immediately benefit from using the SNP detection assay for their investigation of the impact of antimalarial interventions

on the selection of drug-resistant *Plasmodia*. Malaria co-infection with HIV leads to a synergistic interaction that potentially causes increased risk for complications and severity of both diseases. HIV-infected people who are taking cotrimoxazole for chemoprophylaxis are advised to not take SP due to the increased risk of sulfa-mediated adverse reactions. *In vitro* studies have suggested that cotrimoxazole may accelerate the spread of SP resistance (34); However, recent studies have shown that there is a reduced incidence of antifolate resistance among HIV-infected people on cotrimoxazole chemoprophylaxis (30, 44). The PROMOTE study focuses much attention on the use of molecular techniques for the characterization of drug resistance and the selection of resistant parasites in populations that are burdened by both HIV and malaria.

Since the establishment of the UMSP, there have been ongoing efforts to monitor antimalarial drug efficacy. Monthly surveillance reports provide detailed statistics on suspected malaria cases, diagnostic results, and treatment practices in different regions. Given a positive diagnostic result, the two main antimalarials being prescribed are artemisinin-lumefantrine and quinine. The UMSP does not currently report the prevalence of SP resistance, primarily because SP is only used for IPTp among pregnant women. However, surveillance of SP resistance would be informative to policy makers, especially if the transmission of drug-resistant parasites has significantly declined after the drug was withdrawn as front-line treatment. These results are pertinent for the potential re-introduction of SP as front-line treatment of uncomplicated *P. falciparum*.

Uganda is only one of many under-developed countries that are burdened by malaria. These countries lack the infrastructure to collect data from clinical research that enables scientists to characterize the problems associated with disease. National surveillance programs are beneficial to understanding the efficacy of control programs within their country but also within a larger region or transmission zone. As such, Uganda has a history of collaborative surveillance studies with other East African countries. The East African Network for Monitoring Anti-malarial Treatment (EANMAT) and East African Integrated Disease Surveillance Network (EAIDSNet) are just a few examples of collaborative efforts of Ministries of Health for East African countries. Results produced by the EANMAT were quite successful for changing policy based on evidence. For instance, surveillance of declining SP efficacy encouraged policy makers in Burundi to change the front-line therapy from SP to amodiaquine and artesunate combination (17). Activities by the EANMAT are dwindling, however global surveillance programs are growing to fill the void thus created in coordinated responses and routine surveillance.

One important global organization that has been established recently is the Worldwide Antimalarial Resistance Network (WWARN; [www.wwarn.org](http://www.wwarn.org)). WWARN has a key mission of monitoring the emergence and spread of drug-resistant parasites within malarial-endemic regions. Global surveillance programs are becoming easier to establish, simply because the ability to harness and share information is also becoming increasingly easier. WWARN enables researchers to input their study results into an open-access database on antimalarial resistance.

SNPs can then be mapped temporally and geographically, providing regional analysis of trends in drug resistance. The data is open to stakeholders who may want to further investigate poor drug quality or possible replacement of antimalarials used in chemoprophylaxis such as SP-IPTp. WWARN is not limited to molecular marker data, but also includes results from clinical trials, antimalarial quality, pharmacology, and bioinformatics.

The genotyping assay that was developed on the LightCycler® at the University of Alberta can have future implications in providing support with WWARN and their concerted efforts to improve surveillance for a global disease. The assay on the LightCycler® can potentially replace the current genotyping protocol, which would be recognized as a world-wide gold standard for genotyping SP resistance. WWARN is striving to standardize genotyping technologies and protocols; however at the present date, a specific protocol for genotyping for SNPs in the *pfdhfr* and *pfdhps* genes has not yet been implemented (67). This assay would be an important tool for global tracking of SP resistance and monitoring emergence of resistant strains. It could contribute to evidence-based policy-making decisions via the united efforts of WWARN and other agencies to track resistance.

#### **4.2 General conclusions regarding the in-gel technology**

Nanotechnology and microfluidics are revolutionizing point of care (POC) testing. Instrumentation used in molecular surveillance will eventually become miniaturized, which will overcome the need for expensive equipment and highly

trained personnel. Some of the newer methods in microfluidics are dependent upon pressurized systems, channels, and pumps, all of which have energy and financial costs associated, which may not be available in developing countries. To avoid these requirements, PCR can be performed within colloidal hydrogel matrices, a method termed in-gel PCR. The principles for genotyping using melting curve analysis (MCA) of an unlabeled probe can be applied to in-gel technology for point-of-care (POC) testing in resource-limited settings. Although the current platform for the in-gel technology is not operational for the purposes of drug resistance genotyping, there is still a possibility to use the high-throughput method with new versions of the platform. As mentioned in Chapter 3, the Viriloc requires further modifications before genotyping can be performed. Once the Viriloc system is operating at an optimal and consistent level that is similar to the LightCycler®, further work on the genotyping application can be pursued.

#### **4.2.1 Limitations of the system**

The Viriloc system is an inexpensive prototype real-time PCR platform, which is designed to amplify PCR products within polyacrylamide gels. As expected with any prototype instrument, the Viriloc has limitations that hinder optimal amplification and MCA. All future system developments need to consider these limitations, which will be discussed in detail in this section.

Melting curve analysis (MCA) is dependent on the amplification of the PCR products. The PCR itself is dependent on the regulation of heat provided by the Peltier heater. The temperatures set on the Viriloc control this heater; however, the speed at which the Peltier is able to reach the set temperatures,



known as the ramp rate, cannot be controlled. The ramp rate is an important factor in optimizing the PCR efficiency. At low ramp rates, primers bind to each other or to DNA sequences that are not within the amplicon region, thus permitting non-specific amplification of primer-dimers. To add to this problem, the ambient room temperature may further compromise the rate at which the system will reach the denaturing and/or annealing temperature. This could have a major impact on the use of this device in tropical areas.

There are system differences between the Viriloc instruments, as each internal component is made from different manufacturers; this complicates comparing results between the Viriloc systems. As mentioned in Chapter 3, Peltier heaters, cameras, and filters are not uniform across all the Viriloc systems. In the case where a mastermix is split and polymerized in two separate molds and then simultaneously run on two Viriloc systems, different PCR amplification curves and MCA peaks are sometimes but not always produced. For example, one Viriloc has been observed to perform thermal cycling at a faster rate and can generate curves that are “better,” albeit inconsistent from day to day. These “better” curves resemble the MCA curves produced on the LightCycler®. Engineers and researchers are working to identify the source(s) of the observed differences. Current work is in progress to construct a standardized instrument.

#### **4.2.2 Technological requirements for change**

In-gel technology has the potential to deliver genotyping assays for *P. falciparum* to the field. Results from this study have shown that both PCR and MCA for genotyping can be performed within a polyacrylamide gel matrix, as

shown on the LightCycler®. Positive samples from the IPTp study in Uganda will eventually be used for the validation of the genotyping assay using the in-gel PCR technology. Successful validation of the assay using the in-gel technology will encourage field studies to test POC devices in Uganda. The major barrier to genotyping is the platform on which the PCR and MCA are both performed. The researchers who are developing this method and technology are discovering approaches that will allow for multiple SNPs to be measured simultaneously on a single chip directly from blood samples. Once all the configurations of the system are optimized, the in-gel technology will revolutionize molecular surveillance for malaria.

#### **4.2.3 Future implications: application of the technology for use in the field**

Many endemic countries do not have the resources and/or infrastructure to genotype drug-resistant strains using the assay developed on the LightCycler®. There are advantages to using microfluidic platforms for POC testing, especially for endemic areas in low resource settings. Developing a microfluidic device for diagnosing malaria will help to improve the efforts to control the spread of the disease.

The ideal platform will be more sensitive, specific, and cost effective than the gold-standard microscopy. The WHO has created a set of guidelines, known as “ASSURED”, for the development of diagnostic tools for infectious diseases. These tools must encompass the following: (i) affordable, (ii) sensitive, (iii)

specific, (iv) user-friendly, (v) rapid and robust, (vi) equipment-free, and (vii) delivery to those who need it (41, 77).

Although traditional microscopy meets these criteria, it is often not widely available, or microscopists have limited expertise in this technique (87). This method is prone to poor execution, which can be attributed to a number of factors including: poor training, poor quality slide preparation, increased workload, and microscope condition (87). Trained microscopists are skilled in differentiating and identifying the different species of *Plasmodium*. Identification is dependent on lifecycle stage of the parasite and its host tissue (liver versus blood stage). The obvious problem with microscopy for diagnosis is the inability to determine the parasite's genetic make-up that enables its survival in the presence of drugs. In order to improve the diagnostic gold standard, microfluidic platforms need to be portable, adaptable to testing new genomic markers, accurate in detection, and require minimal expertise to operate (41).

There is large support to abandon presumptive treatment of malaria and shift towards parasitological diagnosis. This requires that diagnostic tools are readily available and clinicians are able to interpret results. Sentinel surveillance sites are able to employ rapid diagnostic tests (RDTs) for suspected cases of malaria. These immunochromatographic “dipstick” methods are easy to use, but research has shown that specificity is somewhat compromised. The “dipstick” tests detect antigens (malarial proteins) such as lactate dehydrogenase (pLDH) and histidine-rich protein (HRP II) (25). The overall performance of RDTs are similar to microscopy(32), however the type of RDT used depends on the level of

transmission. High transmission areas should utilize the RDT that is based on the HRPII antigens, whereas low transmission areas should use the RDT that is based on pLDH antigens. HRP2-based RDTs have a high positive predictive value for areas ranging from medium to high transmission. The pLDH-based RDTs are shown to have high specificity but fail to detect subpatent infections, particularly within high transmission areas (32). The objective for using RDTs is to ensure antimalarial treatment is prescribed for patients with malarial infections. Unfortunately, RDTs do not indicate if the infecting parasite has polymorphisms that confer resistance, and this does not suggest to the clinician which type of treatment to provide.

Gene amplification methods are deemed the best alternative for diagnosis compared with RDTs and microscopy. As mentioned previously, these methods require large laboratory infrastructure settings and trained technicians to perform such assays for detection. There are improvements in the field of microfluidics and nanotechnology that are applying high-throughput PCR and MCA assays onto portable devices such that they are easily used in rural environments. One of the first hand-held, real-time PCR platforms to be used in the field was developed by the Lawrence Livermore National Laboratory in 1999. This Handheld Advanced Nucleic Acid Analyzer (HANAA) was directed more for biodefense through its ability to detect various pathogens such as *Bacillus anthracis*, *Yersina pestis*, and *Escherichia spp.*

For more global health applications, Lab-on-a-chip (LOC) research is challenged to provide Western-world technologies for resource-limited settings.

Many of the LOC devices are in the prototype stage of development for closed-loop, miniaturized PCR designs, but most designs are challenged to meet the POC desired characteristics: (i) disposability, (ii) cost-effectiveness, (iii) ease of use and (iv) portability (41).

POC testing has the potential to contribute greatly towards “molecular theranostics,” which is the integration of therapeutics and diagnostics. Essentially, molecular theranostics will utilize genetic information to optimize patient management and disease treatment. *In vivo* and *in vitro* resistance studies have shown associations between treatment failure and the presence of SNPs (76). Thus, case management of malaria can be improved by understanding the genetic makeup of the parasite. The genotyping assay can be applied onto a POC device to build a multi-parameter platform that can detect the multiple SNPs for the *dhfr* and *dhps* genes. Researchers and clinicians can apply this information to estimate the risk of treatment failure due to parasitological resistance. With respect to theranostics, the cumulative SNPs detected by POC testing will inform clinicians on the appropriateness to treat with a particular antimalarial.

The POC device can also be developed for speciation of *Plasmodia*. There are five different species of *Plasmodia* that are able to cause illness in humans. Effectiveness of treatment is dependent upon the type of infecting species. Much like detecting the presence of polymorphisms associated with resistance, determining the infecting species will direct clinicians in the appropriateness of treatment. Treatment is primarily to control for *P. falciparum*, but in the case when *P. vivax* or *P. ovale* are confirmed by diagnosis, patients are usually treated

with primaquine. There are contraindications to providing primaquine, such as when a person is characterized with glucose-6-phosphate dehydrogenase deficiency (G6PD). Oxidative drugs, such as primaquine, cause acute hemolysis in patients and eventually lead to the onset of hyperbilirubinemia. G6PD deficiency can be determined either by rapid fluorescent spot tests or detection of specific mutations using PCR. An ideal POC platform would be able to determine if a patient has contraindications to certain antimalarials. This would help to ensure that the prescribed antimalarial is functioning at its optimal capacity without severe adverse effects.

One problem encountered with the use of RDTs is the appropriate response to negative results. The overlapping symptoms of malaria with other febrile illnesses mean it is essential to ensure that people do not receive antimalarials if their test result is negative for the presence of *P. falciparum*. There are circumstances under which a person receives an antimalarial despite receiving a negative result from a RDT. In areas where malaria is not the only cause for febrile disease, other tests are needed to distinguish among the illnesses that cause febrile symptoms. Currently, such a fever-type panel is not available, but it would make a significant contribution to the clinical management of fever. Furthermore, the provision of antimalarials would not be haphazardly distributed, which would lower the spread of resistance through effective malaria management in endemic areas.

Future improvements in malaria control will rely upon POC devices, which will bridge the gap between testing in rural areas and that which is

performed in advanced laboratory settings. More importantly, POC testing will fundamentally reduce misdiagnosis due to syndromic management, which will in turn lead to reductions in wasted resources and antimalarial resistance. At the surveillance level, POC testing will contribute important evidence necessary for policy change.

## References

1. **Achan, J., A. O. Talisuna, A. Erhart, A. Yeka, J. K. Tibenderana, F. N. Baliraine, P. J. Rosenthal, and U. D'Alessandro.** 2011. Quinine, an old anti-malarial drug in a modern world: role in the treatment of malaria. *Malar J* **10**:144.
2. **Alker, A. P., J. J. Juliano, S. R. Meshnick, A. Owen, E. Ochong, D. J. Bell, D. J. Johnson, U. d'Alessandro, M. Mulenga, S. Muangnoicharoen, J. P. Van Geertruyden, P. A. Winstanley, P. G. Bray, and S. A. Ward.** 2009. *Plasmodium falciparum* and dihydrofolate reductase I164L mutations in Africa. *Antimicrob Agents Chemother* **53**:1722-1723.
3. **Alker, A. P., V. Mwapasa, and S. R. Meshnick.** 2004. Rapid real-time PCR genotyping of mutations associated with sulfadoxine-pyrimethamine resistance in *Plasmodium falciparum*. *Antimicrob Agents Chemother* **48**:2924-2929.
4. **Alker, A. P., V. Mwapasa, A. Purfield, S. J. Rogerson, M. E. Molyneux, D. D. Kamwendo, E. Tadesse, E. Chaluluka, and S. R. Meshnick.** 2005. Mutations associated with sulfadoxine-pyrimethamine and chlorproguanil resistance in *Plasmodium falciparum* isolates from Blantyre, Malawi. *Antimicrob Agents Chemother* **49**:3919-3921.
5. **Andriantsoanirina, V., V. Lascombes, A. Ratsimbaoa, C. Bouchier, J. Hoffman, M. Tichit, L.-P. Rabarijaona, R. Durand, and D. Ménard.** 2009. Rapid detection of point mutations in *Plasmodium falciparum* genes associated with antimalarial drugs resistance by using High-Resolution Melting analysis. *J Microbiol Methods* **78**:165-170.
6. **Atrazhev, A., D. Manage, A. Stickel, H. Crabtree, L. Pilarski, and J. Acker.** 2010. In-Gel technology for PCR genotyping and pathogen detection. *Anal Chem* **82**:572-581.
7. **Augustine, A. D., B. F. Hall, W. W. Leitner, A. X. Mo, T. M. Wali, and A. S. Fauci.** 2009. NIAID workshop on immunity to malaria: addressing immunological challenges. *Nature Immunol* **10**:673-678.
8. **Bacon, D. J., D. Tang, C. Salas, N. Roncal, C. Lucas, L. Gerena, L. Tapia, A. A. Llanos-Cuentas, C. Garcia, L. Solari, D. Kyle, and A. J. Magill.** 2009. Effects of point mutations in *Plasmodium falciparum* dihydrofolate reductase and dihydropterate synthase genes on clinical outcomes and in vitro susceptibility to sulfadoxine and pyrimethamine. *PLoS ONE* **4**:e6762.
9. **Barnes, K. I., and N. J. White.** 2005. Population biology and antimalarial resistance: The transmission of antimalarial drug resistance in *Plasmodium falciparum*. *Acta Trop* **94**:230-240.
10. **Basco, L. K., R. Tahar, and P. Ringwald.** 1998. Molecular basis of *in vivo* resistance to sulfadoxine-pyrimethamine in African adult patients infected with *Plasmodium falciparum* malaria parasites. *Antimicrob Agents Chemother* **42**:1811-1814.



11. **Bate, R., P. Coticelli, R. Tren, and A. Attaran.** 2008. Antimalarial drug quality in the most severely malarious parts of Africa - A six country study. *PLoS ONE* **3**:e2132.
12. **Bloand, P. B., and WHO.** 2001. Drug resistance in malaria. World Health Organization Geneva, Switzerland.
13. **Bustamante, C., C. N. Batista, and M. Zalis.** 2009. Molecular and biological aspects of antimalarial resistance in *Plasmodium falciparum* and *Plasmodium vivax*. *Curr Drug Targets* **10**:279-90.
14. **Chico, R. M., and D. Chandramohan.** Intermittent preventive treatment of malaria in pregnancy: at the crossroads of public health policy. *Tropical Medicine & International Health*.
15. **Clyde, D. F., and G. T. Shute.** 1957. Resistance of *Plasmodium falciparum* in Tanganyika to pyrimethamine administered at weekly intervals. *Trans R Soc Trop Med Hyg* **51**:505-513.
16. **Cruz, R. E., S. E. Shokoples, D. P. Manage, and S. K. Yanow.** 2010. High-Throughput genotyping of single nucleotide polymorphisms in the *Plasmodium falciparum* dhfr gene by asymmetric PCR and melt-curve analysis. *J Clin Microbiol* **48**:3081-3087.
17. **D'Alessandro, U.** 2003. The efficacy of antimalarial monotherapies, sulphadoxine-pyrimethamine and amodiaquine in East Africa: implications for sub-regional policy. *Trop Med Int Health* **8**:860-867.
18. **Daily, J. P.** 2006. Antimalarial drug therapy: the role of parasite biology and drug resistance. *J Clin Pharmacol* **46**:1487-1497.
19. **de Villiers, K. A., H. M. Marques, and T. J. Egan.** 2008. The crystal structure of halofantrine-ferriporphyrin IX and the mechanism of action of arylmethanol antimalarials. *J Inorg Biochem* **102**:1660-1667.
20. **Decuyper, S., E. Elinck, C. Van Overmeir, A. Talisuna, U. D'Alessandro, and J. Dujardin.** 2003. Pathogen genotyping in polyclonal infections: application of a fluorogenic polymerase-chain-reaction assay in malaria. *J Infect Dis* **188**:1245 - 1249.
21. **Enayati, A., and J. Hemingway.** 2010. Malaria management: past, present, and future. *Annu Rev Entomol* **55**:569-591.
22. **Fitch, C. D.** 2004. Ferriporphyrin IX, phospholipids, and the antimalarial actions of quinoline drugs. *Life Sci* **74**:1957-1972.
23. **Foley, M., and L. Tilley.** 1997. Quinoline antimalarials: mechanisms of action and resistance. *Int J Parasitol* **27**:231-240.
24. **Garritano, S., F. Gemignani, C. Voegelé, T. Nguyen-Dumont, F. Le Calvez-Kelm, D. De Silva, F. Lesueur, S. Landi, and S. V. Tavtigian.** 2009. Determining the effectiveness of High Resolution Melting analysis for SNP genotyping and mutation scanning at the TP53 locus. *BMC Genet* **10**.
25. **Gascoyne, P., J. Satayavivad, and M. Ruchirawat.** 2004. Microfluidic approaches to malaria detection. *Acta Trop* **89**:357-369.
26. **Goodman, C., W. Brieger, A. Unwin, A. Mills, S. Meek, and G. Greer.** 2007. Medicine sellers and malaria treatment in sub-Saharan Africa: what

- do they do and how can their practice be improved? *Am J Trop Med Hyg* **77**:203-218.
27. **Greenberg, J., and E. M. Richeson.** 1950. Potentiation of the antimalarial activity of sulfadiazine by 2,4-diamino-5-aryloxyrimidines. *J Pharmacol Exp Ther* **99**:444-449.
  28. **Gregson, A., and C. V. Plowe.** 2005. Mechanisms of resistance of malaria parasites to antifolates. *Pharmacol Rev* **57**:117-45.
  29. **Habalová, V., L. Klimčáková, J. Zidzik, and I. Tkáč.** 2009. Rapid and cost effective genotyping method for polymorphisms in PPARG, PPARGC1 and TCF7L2 genes. *Mol Cell Probes* **23**:52-54.
  30. **Hamer, D. H., and C. J. Gill.** 2008. Balancing individual benefit against public health risk: the impact of cotrimoxazole prophylaxis in HIV-infected patients on antimicrobial resistance. *Am J Trop Med Hyg* **79**:299-300.
  31. **Harrington, W., T. Mutabingwa, A. Muehlenbachs, B. Sorensen, M. Bolla, M. Fried, and P. Duffy.** 2009. Competitive facilitation of drug-resistant *Plasmodium falciparum* malaria parasites in pregnant women who receive preventive treatment. *Proc Natl Acad Sci U S A* **106**:9027-9032.
  32. **Hopkins, H., L. Bebell, W. Kambale, C. Dokomajilar, P. J. Rosenthal, and G. Dorsey.** 2008. Rapid diagnostic tests for malaria at sites of varying transmission intensity in Uganda. *J Infect Dis* **197**:510-518.
  33. **Hyde, J. E.** 2005. Exploring the folate pathway in *Plasmodium falciparum*. *Acta Trop* **94**:191-206.
  34. **Iyer, J. K., W. K. Milhous, J. F. Cortese, J. G. Kublin, and C. V. Plowe.** 2001. *Plasmodium falciparum* crossresistance between trimethoprim and pyrimethamine. *Lancet* **358**:1066-1067.
  35. **Jiang, H., N. Li, V. Gopalan, M. M. Zilversmit, S. Varma, V. Nagarajan, J. Li, J. Mu, K. Hayton, and B. Henschen.** 2011. High recombination rates and hotspots in a *Plasmodium falciparum* genetic cross. *Genome Biol* **12**:R33.
  36. **Klein, D.** 2002. Quantification using real-time PCR technology: applications and limitations. *Trends Mol Med* **8**:257-260.
  37. **Kristensen, L. S., and A. Dobrovic.** 2008. Direct genotyping of single nucleotide polymorphisms in methyl metabolism genes using probe-free high-resolution melting analysis. *Cancer Epidemiol Biomarkers Prev* **17**:1240-1247.
  38. **Kublin, J., J. Cortese, E. Njunju, R. Mukadam, J. Wirima, P. Kazembe, A. Djimdè, B. Kouriba, T. Taylor, and C. Plowe.** 2003. Reemergence of chloroquine-sensitive *Plasmodium falciparum* malaria after cessation of chloroquine use in Malawi. *J Infect Dis* **187**:1870-1875.
  39. **Kublin, J. G., F. K. Dzinjalama, D. D. Kamwendo, E. M. Malkin, J. F. Cortese, L. M. Martino, R. A. G. Mukadam, S. J. Rogerson, A. G. Lescano, M. E. Molyneux, P. A. Winstanley, P. Chimpeni, T. E. Taylor, and C. V. Plowe.** 2002. Molecular markers for failure of

- sulfadoxine-pyrimethamine and chlorproguanil-dapsone treatment of *Plasmodium falciparum* malaria. *J Infect Dis* **185**:380-388.
40. **Laufer, M. K., P. C. Thesing, N. D. Eddington, R. Masonga, F. K. Dzinjalama, S. L. Takala, T. E. Taylor, and C. V. Plowe.** 2006. Return of chloroquine antimalarial efficacy in Malawi. *N Engl J Med* **355**:1959-1966.
  41. **Lee, W. G., Y. G. Kim, B. G. Chung, U. Demirci, and A. Khademhosseini.** 2010. Nano/Microfluidics for diagnosis of infectious diseases in developing countries. *Adv Drug Deliv Rev* **62**:449-457.
  42. **Lumb, V., M. K. Das, P. Mitra, A. Ahmed, M. Kumar, P. Kaur, A. P. Dash, S. S. Singh, and Y. D. Sharma.** 2009. Emergence of an unusual sulfadoxine-pyrimethamine resistance pattern and a novel K540N mutation in dihydropteroate synthetase in *Plasmodium falciparum* isolates obtained from car Nicobar Island, India, after the 2004 Tsunami. *J Infect Dis* **199**:1064-1073.
  43. **Maitarad, P., P. Saparpakorn, S. Hannongbua, S. Kamchonwongpaisan, B. Tarnchompoo, and Y. Yuthavong.** 2009. Particular interaction between pyrimethamine derivatives and quadruple mutant type dihydrofolate reductase of *Plasmodium falciparum*: CoMFA and quantum chemical calculations studies. *J Enzyme Inhib Med Chem* **24**:471-479.
  44. **Malamba, S. S., J. Mermin, A. Reingold, J. R. Lule, R. Downing, R. Ransom, A. Kigozi, B. M. Hunt, A. Hubbard, P. J. Rosenthal, and G. Dorsey.** 2006. Effect of cotrimoxazole prophylaxis taken by human immunodeficiency virus (HIV) infected persons on the selection of sulfadoxine-pyrimethamine resistant malaria parasites among HIV-uninfected household members. *Am J Trop Med Hyg* **75**:375-380.
  45. **Malisa, A. L., R. J. Pearce, S. Abdulla, H. Mshinda, P. S. Kachur, P. Bloland, and C. Roper.** 2010. Drug coverage in treatment of malaria and the consequences for resistance evolution- evidence from the use of sulphadoxine/pyrimethamine. *Malar J* **9**:190-190.
  46. **May, J., and C. G. Meyer.** 2003. Chemoresistance in falciparum malaria. *Trends Parasitol* **19**:432-435.
  47. **McCollum, A. M., A. C. Poe, M. Hamel, C. Huber, Z. Zhou, Y. P. Shi, P. Ouma, J. Vulule, P. Bloland, L. Slutsker, J. W. Barnwell, V. Udhayakumar, and A. A. Escalante.** 2006. Antifolate resistance in *Plasmodium falciparum*: multiple origins and identification of novel dhfr alleles. *J Infect Dis* **194**:189-97.
  48. **McGready, R., N. White, and F. Nosten.** 2011. Parasitological efficacy of antimalarials in the treatment and prevention of falciparum malaria in pregnancy 1998 to 2009: a systematic review. *BJOG* **118**:123-135.
  49. **Mens, P. F., C. van Overmeir, M. Bonnet, J. C. Dujardin, and U. d'Alessandro.** 2008. Real-time PCR/MCA assay using fluorescence resonance energy transfer for the genotyping of resistance related DHPS-540 mutations in *Plasmodium falciparum*. *Malar J* **7**:48.

50. **Mockenhaupt, F. P., G. Bedu-Addo, T. A. Eggelte, L. Hommerich, V. Holmberg, C. von Oertzen, and U. Bienzle.** 2008. Rapid increase in the prevalence of sulfadoxine-pyrimethamine resistance among *Plasmodium falciparum* isolated from pregnant women in Ghana. *J Infect Dis* **198**:1545-1549.
51. **Montgomery, J., C. T. Wittwer, R. Palais, and L. Zhou.** 2007. Simultaneous mutation scanning and genotyping by high-resolution DNA melting analysis. *Nat Protoc* **2**:59-66.
52. **Mwai, L., E. Ochong, A. Abdirahman, S. M. Kiara, S. Ward, G. Kokwaro, P. Sasi, K. Marsh, S. Borrmann, and M. Mackinnon.** 2009. Chloroquine resistance before and after its withdrawal in Kenya. *Malar J* **8**:106.
53. **Nosten, F., R. McGready, U. d'Alessandro, A. Bonell, F. Verhoeff, C. Menéndez, T. Mutabingwa, and B. Brabin.** 2006. Antimalarial drugs in pregnancy: a review. *Curr Drug Saf* **1**:1-15.
54. **Nuwaha, F.** 2001. The challenge of chloroquine-resistant malaria in sub-Saharan Africa. *Health Policy Plan* **16**:1.
55. **Nyunt, M., I. Adam, K. Kayentao, J. Van Dijk, P. Thuma, K. Mauff, F. Little, Y. Cassam, E. Guirou, and B. Traore.** 2009. Pharmacokinetics of sulfadoxine and pyrimethamine in intermittent preventive treatment of malaria in pregnancy. *Clin Pharmacol Ther* **87**:226-234.
56. **O'Meara, W. P., D. L. Smith, and F. E. McKenzie.** 2006. Potential impact of intermittent preventive treatment (IPT) on spread of drug-resistant malaria. *PLoS Med* **3**:e141.
57. **Ochong, E., D. J. Bell, D. J. Johnson, U. D'Alessandro, M. Mulenga, S. Muangnoicharoen, P. A. Winstanley, P. G. Bray, S. A. Ward, and A. Owen.** 2008. *Plasmodium falciparum* harbouring DHFR I164L are absent in Malawi and Zambia even under antifolate drug pressure. *Antimicrob Agents Chemother*:AAC.00431-08.
58. **Olliaro, P.** 2001. Mode of action and mechanisms of resistance for antimalarial drugs. *Pharmacol Ther* **89**:207-219.
59. **Parikh, S., and P. J. Rosenthal.** 2010. Intermittent preventive therapy for malaria in pregnancy: is sulfadoxine-pyrimethamine the right drug? *Clin Pharmacol Ther* **87**:160-162.
60. **Payne, D.** 1988. Did medicated salt hasten the spread of chloroquine resistance in *Plasmodium falciparum*? *Parasitol Today* **4**:112-115.
61. **Petersen, I., R. Eastman, and M. Lanzer.** 2011. Drug-resistant malaria: molecular mechanisms and implications for public health. *FEBS Lett* **585**:1551-1562.
62. **Peterson, D. S., W. K. Milhous, and T. E. Wellems.** 1990. Molecular basis of differential resistance to cycloguanil and pyrimethamine in *Plasmodium falciparum* malaria. *Proc Natl Acad Sci U S A* **87**:3018-3022.
63. **Pfeiffer, K., F. Some, O. Müller, A. Sie, B. Kouyaté, W. E. Haefeli, A. Zoungrana, L. L. Gustafsson, G. Tomson, and R. Sauerborn.** 2008. Clinical diagnosis of malaria and the risk of chloroquine self-medication in rural health centres in Burkina Faso. *Trop Med Int Health* **13**:418-426.

64. **Picot, S., P. Olliaro, F. De Monbrison, A. L. Bienvenu, R. N. Price, and P. Ringwald.** 2009. A systematic review and meta-analysis of evidence for correlation between molecular markers of parasite resistance and treatment outcome in falciparum malaria. *Malar J* **8**.
65. **Plowe, C. V.** 2003. Monitoring antimalarial drug resistance: making the most of the tools at hand. *J Exp Biol* **206**:3745-3752.
66. **Plowe, C. V., J. F. Cortese, A. Djimde, O. C. Nwanyanwu, W. M. Watkins, P. A. Winstanley, J. G. Estrada-Franco, R. E. Mollinedo, J. C. Avila, J. L. Cespedes, D. Carter, and O. K. Doumbo.** 1997. Mutations in *Plasmodium falciparum* dihydrofolate reductase and dihydropteroate synthase and epidemiologic patterns of pyrimethamine-sulfadoxine use and resistance. *J Infect Dis* **176**:1590-6.
67. **Plowe, C. V., C. Roper, J. W. Barnwell, C. T. Happi, H. H. Joshi, W. Mbacham, S. R. Meshnick, K. Mugittu, I. Naidoo, and R. N. Price.** 2007. World Antimalarial Resistance Network(WARN) III: Molecular markers for drug resistant malaria. *Malar J* **6**:121.
68. **Righetti, P. G., and C. Gelfi.** 1997. Electrophoresis gel media: the state of the art. *J Chromatogr B Biomed Sci Appl* **699**:63-75.
69. **Schapira, A., I. C. Bygbjerg, S. Jepsen, H. Flachs, and M. W. Bentzon.** 1986. The susceptibility of *Plasmodium Falciparum* to sulfadoxine and pyrimethamine: correlation of *in vivo* and *in vitro* Results. *Am J Trop Med Hyg* **35**:239-245.
70. **Schlitzer, M.** 2007. Malaria chemotherapeutics part I: history of antimalarial drug development, currently used therapeutics, and drugs in clinical development. *ChemMedChem* **2**:944-986.
71. **Sempala, S. D. K.** 2002. Institute profile: the Uganda Virus Research Institute. *Trends Microbiol* **10**:346-348.
72. **Sevene, E., R. González, and C. Menéndez.** 2010. Current knowledge and challenges of antimalarial drugs for treatment and prevention in pregnancy. *Expert Opin Pharmacother* **11**:1277-1293.
73. **Shokoples, S. E., M. Ndao, K. Kowalewska-Grochowska, and S. K. Yanow.** 2009. Multiplexed real-time PCR assay for discrimination of *Plasmodium* species with improved sensitivity for mixed infections. *J Clin Microbiol* **47**:975-80.
74. **Souares, A., R. Lalou, I. Sene, D. Sow, and J.-Y. Le Hesran.** 2008. Adherence and effectiveness of drug combination in curative treatment among children suffering uncomplicated malaria in rural Senegal. *Trans R Soc Trop Med Hyg* **102**:751-758.
75. **Sserwanga, A., J. C. Harris, R. Kigozi, M. Menon, H. Bukirwa, A. Gasasira, S. Kakeeto, F. Kizito, E. Quinto, D. Rubahika, S. Nasr, S. Filler, M. R. Kamya, and G. Dorsey.** 2011. Improved malaria case management through the Implementation of a health facility-based sentinel site surveillance system in Uganda. *PLoS ONE* **6**:e16316.
76. **Talisuna, A. O., P. Bloland, and U. D'Alessandro.** 2004. History, dynamics, and public health importance of malaria parasite resistance. *Clin Microbiol Rev* **17**:235-254.

77. **Urdea, M., L. A. Penny, S. S. Olmsted, M. Y. Giovanni, P. Kaspar, A. Shepherd, P. Wilson, C. A. Dahl, S. Buchsbaum, and G. Moeller.** 2006. Requirements for high impact diagnostics in the developing world. *Nature* **444**:73-79.
78. **Vafa, M., M. Troye-Blomberg, J. Anchang, A. Garcia, and F. Migot-Nabias.** 2008. Multiplicity of *Plasmodium falciparum* infection in asymptomatic children in Senegal: relation to transmission, age and erythrocyte variants. *Malar J* **7**.
79. **White, N.** 2004. Antimalarial drug resistance. *J Clin Invest* **113**:1084-1092.
80. **White, N.** 2002. The assessment of antimalarial drug efficacy. *Trends Parasitol* **18**:458-464.
81. **White, N.** 2005. Intermittent presumptive treatment for malaria. *PLoS Med* **2**:e3.
82. **WHO.** 2010. Guidelines for the treatment of malaria. World Health Organization.
83. **WHO.** 2001. Roll back malaria: the use of antimalarial drugs. World Health Organization.
84. **WHO.** 2009. World malaria report 2009. World Health Organization.
85. **Wilson, P. E., A. P. Alker, and S. R. Meshnick.** 2005. Real-time PCR methods for monitoring antimalarial drug resistance. *Trends Parasitol* **21**:278-83.
86. **Wilson, P. E., W. Kazadi, D. D. Kamwendo, V. Mwapasa, A. Purfield, and S. R. Meshnick.** 2005. Prevalence of pfcr mutations in Congolese and Malawian *Plasmodium falciparum* isolates as determined by a new Taqman assay. *Acta Trop* **93**:97-106.
87. **Wongsrichanalai, C., M. J. Barcus, S. Muth, A. Sutamihardja, and W. H. Wernsdorfer.** 2007. A review of malaria diagnostic tools: microscopy and rapid diagnostic test (RDT). *Am J Trop Med Hyg* **77**:119-127.
88. **Wongsrichanalai, C., A. L. Pickard, W. H. Wernsdorfer, and S. R. Meshnick.** 2002. Epidemiology of drug-resistant malaria. *Lancet Infect Dis* **2**:209-18.
89. **Yanow, S. K., L. A. Purcell, and T. W. Spithill.** 2006. The A/T-specific DNA alkylating agent adozelesin inhibits *Plasmodium falciparum* growth in vitro and protects mice against *Plasmodium chabaudi adami* infection. *Mol Biochem Parasitol* **148**:52-9.
90. **Yuvaniyama, J., P. Chitnumsub, S. Kamchonwongpaisan, J. Vanichtanankul, W. Sirawaraporn, P. Taylor, M. D. Walkinshaw, and Y. Yuthavong.** 2003. Insights into antifolate resistance from malarial DHFR-TS structures. *Nat Struct Mol Biol* **10**:357-365.
91. **Zhang, K., and P. K. Rathod.** 2002. Divergent regulation of dihydrofolate reductase between malaria parasite and human host. *Science* **296**:545-7.

92. **Zhou, Z., A. C. Poe, J. Limor, K. K. Grady, I. Goldman, A. M. McCollum, A. A. Escalante, J. W. Barnwell, and V. Udhayakumar.** 2006. Pyrosequencing, a high-throughput method for detecting single nucleotide polymorphisms in the dihydrofolate reductase and dihydropteroate synthetase genes of *Plasmodium falciparum*. *J Clin Microbiol* **44**:3900-3910.

## Appendix 1: Glossary

**Early treatment failure:** Development of danger signs or severe malaria on days 1-3 in the presence of parasitemia; parasitemia on day 3 with axillary temperature greater than 37.5 °C (28).

**Gametocytes:** The sexual forms of *Plasmodia* that differentiate from the merozoites. This sexual stage is transmitted to the mosquito where parasites undergo sexual reproduction.

**Late clinical failure:** Development of danger signs or severe malaria after day 3 in the presence of parasitemia, without previously meeting any of the criteria of early treatment failure (28).

**Late parasitological failure:** Presence of parasitemia from day 7 to day 28 and axillary temperature greater than 37.5 °C without previously meeting any of the criteria of early treatment failure or late clinical failure (28).

**Peltier heater:** a device used for thermal cycling, which allows for heat to move from one side to the other as current runs through the device.

**Polymerase chain reaction (PCR):** Process of DNA amplification through multiple cycles of heating and cooling. Each cycle consists of a denaturation, annealing, and extension step.

**Schizonts:** A multinucleated cell stage during the asexual phase of the *Plasmodia* lifecycle. Each infected red blood cell is capable of generating 12-16 merozoites.

**Single nucleotide polymorphisms:** Variation in the DNA sequence whereby a single nucleotide (either a purine or pyrimidine) has been replaced by another nucleotide.

**Trophozoites:** The form of the parasite that is in the metabolically active growth stage.